THERMALLY ACTIVATED FLOW AND STRAIN RATE HISTORY EFFECTS FOR SOME POLY-CRYSTALLINE FCC METALS

J. Klepaczko

Brown University

Prepared for:

Army Research Office-Durham

March 1974

Unclassified

Security Classification

AD-781 222

DOCUMENT CONTROL DATA – R & D

(Security classification of title, body of abstract and indexing annotation must be entered when the overall report is classified)

1. ORIGINATING ACTIVITY (Corporate author)
Division of Engineering - Brown University
Providence, R. I. 02912

2a. REPORT SECURITY CLASSIFICATION
unclassified

2b. GROUP

3. REPORT TITLE
Thermally Activated Flow and Strain Rate History Effects for Some Polycrystalline FCC Metals

4. DESCRIPTIVE NOTES (Type of report and inclusive dates)
technical report March 1974

5. AUTHOR(S) (First name, middle initial, last name)
J. Klepaczko

6. REPORT DATE	7a. TOTAL NO. OF PAGES	7b. NO. OF REFS
March, 1974	42	35

8a. CONTRACT OR GRANT NO.	9a. ORIGINATOR'S REPORT NUMBER(S)
DA-ARO-D-31-124-73-G182	ARO-D-G182/27
b. PROJECT NO.	
c.	9b. OTHER REPORT NO(S) (Any other numbers that may be assigned this report)
d.	

10. DISTRIBUTION STATEMENT
Approved for public release; distribution unlimited

11. SUPPLEMENTARY NOTES	12. SPONSORING MILITARY ACTIVITY
	U. S. Army Research Office - Durham Box CM, Duke Station Durham, N. C. 27706

13. ABSTRACT

It is shown in the paper that the strain rate history effects play a very important role in the plastic behavior of polycrystalline fcc metals. These effects are attributed to some differences in the effective dislocation multiplication rates at different strain rates. A mathematical description of the effects discussed is possible by a coupling of two relationships. One of these is the relation resulting from the thermally activated process which is dominating at a certain level of strain, while the second is of an evolutionary type. An evolutionary relationship describes the changes in structure during the course of plastic deformation. A few examples of an evolutionary relationship along with a thermally activated intersection model are discussed. Combination of these two models lead to a more general constitutive equation, namely

$$\tau = \tau_A(t,T) + \tau^*(\dot{\gamma},T)$$

where $\tau_A(t,T)$ is the time and temperature dependent athermal component of stress, $\tau^*(\dot{\gamma},T)$ is the strain rate and temperature dependent thermally activated component of stress. Also, some specific cases of such an evolutionary relationship are discussed. Such an approach is applicable in the solution of many important engineering problems involving rapid changes of strain rates during course of plastic deformation.

DD FORM 1 NOV 65 1473

Unclassified

Security Classification

14. KEY WORDS	LINK A		LINK B		LINK C	
	ROLE	WT	ROLE	WT	ROLE	WT
Strain Rate History						
FCC Metals						
Dislocations						
Thermal Activation						
Plastic Deformation						

ABSTRACT

It is shown in the paper that the strain rate history effects play a very important role in the plastic behavior of polycrystalline fcc metals. These effects are attributed to some differences in the effective dislocation multiplication rates at different strain rates. A mathematical description of the effects discussed is possible by a coupling of two relationships. One of these is the relation resulting from the thermally activated process which is dominating at a certain level of strain, while the second is of an evolutionary type. An evolutionary relationship describes the changes in structure during the course of plastic deformation. A few examples of an evolutionary relationship along with a thermally activated intersection model are discussed. Combination of these two models lead to a more general constitutive equation, namely

$$\tau = \tau_A(t,T) + \tau^*(\dot{\gamma},T)$$

where $\tau_A(t,T)$ is the time and temperature dependent athermal component of stress, $\tau^*(\dot{\gamma}, T)$ is the strain rate and temperature dependent thermally activated component of stress. Also, some specific cases of such an evolutionary relationship are discussed. Such an approach is applicable in the solution of many important engineering problems involving rapid changes of strain rates during course of plastic deformation.

THERMALLY ACTIVATED FLOW AND STRAIN RATE HISTORY EFFECTS FOR SOME POLYCRYSTALLINE FCC METALS

J. Klepaczko*

Division of Engineering, Brown University, Providence, U.S.A.

1. Experimental Evidence of Strain Rate History Effects for FCC Metals.

The mechanical behavior of metals and alloys deformed plastically at different rates of strain and temperatures has been extensively studied during the last decade. Most of the results relate to tests at a constant strain rate or temperature. Moreover, the current value of the flow stress depends on the past history of deformation, giving rise to strain rate or temperature history effects. Temperature history effects for aluminum and copper were reported earlier than rate history effects[1,2]. The recent experimental data for aluminum, [3,4,5,6,11] aluminum alloys[10], copper[7,9,11,12] and lead [8], which were obtained by a sudden increase or decrease of the strain rate, point out clearly that the flow stress of these metals depends not only on the instantaneous values of the strain rate, but also depends on their strain rate histories. It then appears that the influence of strain rate and temperature on the stress-strain relationship for polycrystalline fcc metals is more complicated than would be deduced on the basis of a constant rate or constant temperature test. A slightly different dislocation structure is developed after low or high strain rate deformation of a metal to the same level of plastic strain. The same situation is true for the process of plastic deformation at different temperatures. This shows that the flow stress is not a unique function of strain, strain rate and temperature.

For polycrystalline fcc metals incremental tests provide results such as those shown schematically in Fig. 1 in which shear components of stress and strain are plotted. The lowest curve in Fig. 1(a) represents a portion of the stress--

* On leave from Institute of Fundamental Technological Research, Warsaw, Poland.

strain relation obtained during straining at a relatively low strain rate, say $\dot{\gamma}_i = 10^{-4}\ s^{-1}$ or $10^{-5} s^{-1}$, while the upper curve is for a high strain rate, say $\dot{\gamma}_r = 10^{2\ -1}$ or $10^{3} s^{-1}$. On the other hand, a specimen can be loaded at one strain rate $\dot{\gamma}_i$ up to a strain γ_i at which point the strain rate is increased suddenly to $\dot{\gamma}_r$. Such a strain rate history is shown in Fig. 1(c). It results in the stress-strain curve in Fig. 1(a) which follows the path ABCD. A similar path is followed when a specimen is loaded at a single constant strain rate if it suffers a sharp drop in temperature at γ_i. A schematic picture for the strain rate decrease or increase of temperature is shown in Fig. 1(b) and Fig. 1(d).

Considerable improvements have been achieved in the last decade in the experimental techniques used to test metals under dynamic conditions. These have produced more reliable results especially for the incremental type experiments in the high strain rate region. The most effective type of experiment is performed under pure shear conditions, in which thin tubular specimens are used together with a modified torsional split-Hopkinson bar [6,11,13]. The results of incremental tests for 1100-0 aluminum, shown in Fig. 2, were obtained using the torsional split-Hopkinson bar technique.[6] The nominal strain rate of $8.5 \times 10^{2}\ s^{-1}$ in shear is superimposed within a very short rise time (~10μs) with no unloading on a slow initial strain rate of $5 \times 10^{-5}\ s^{-1}$. The increment in strain rate is imposed at a previously selected value of shear strain γ_i within a range up to $\gamma_i = 0.15$. These results are quite similar to the schematic picture in Fig. 1(a). The only difference in appearance comes in the presence of an upper and lower yield stress in the initial portion of the incremental stress-strain diagram.

Since the effect of increments in strain rate on the shape of the stress-strain diagram for copper was unknown, strain rate incremental tests were under-

taken on this metal[9]. Again, the split-Hopkinson bar technique was used, and the final results of these experiments is shown in Fig. 3. Each incremental curve on this diagram represents at least three tests. These experimental results are shown partly as dotted lines to indicate that the strain rate is not constant during the entire incremental test: it is increasing at a nearly linear rate to the final maximum value during the initial part of the incremental curve which is shown dotted. The solid lines indicate that the strain rate has attained a value of about $(9\pm1) \times 10^{2}\ s^{-1}$ during that portion of the incremental test. Since the split-Hopkinson bar technique is not adequate to measure the exact initial elastic response of the specimen, these responses are assumed to be elastic with the shear modulus G. The estimated elastic increments of stress, which take place at a shear strain rate of about $3.5 \times 10^{2}\ s^{-1}$, are shown above the low strain rate curve. It may be noted that the initial strain rate $\dot{\gamma}_i$ for these experiments is about $2.2 \times 10^{-3}\ s^{-1}$. It is evident from Fig. 3 that strain rate history effects are also present in copper.

Comparison of the results in Fig. 3 obtained for copper with those for aluminum, which are shown in Fig. 2, reveals a great similarity in the whole behavior of these metals. The only difference is in the upper and lower yield point which is observed in aluminum but not in the case of copper. It may be noted here that similar strain rate history effects were observed in lead of room temperature[8].

These observations support the idea that in the case of polycrystalline fcc metals the dislocation processes responsible for temperature history and strain rate history effects are similar.

Thus, there is a need to relate such macroscopic behavior to its corresponding microscopic structure. The main problem is the lack of a detailed understanding of the mechanisms for strain hardening of polycrystalline aggregates

of fcc metals and their influence on strain rate and temperature behavior. Strong evidence is now available supporting the supposition that the strain rate and temperature behavior is related to specific thermally activated dislocation mechanisms. However, less evidence exists as to how these mechanisms depend on the strain hardened state of metals. In the latter part of this paper an explanation will be offered concerning this question.

2. Thermal Activation Strain Rate Analysis

A very straightforward way to explain some fundamental features of the strain rate and temperature history effects is to apply the thermal activation strain rate analysis. This is a formal approach in which the basic constitutive relation is derived on the basis of thermodynamics of rate theory. The formalism lies in the averaging process which implies that in the constitutive relation all physical quantities such as the length of an element of a dislocation line which is pinned between obstacles, its glide velocity, the free energy of activation, the effective stress, and the activation area, are simply recognized as average values, but the process of averaging is mathematically unspecified. In some cases the resulting averaged parameters can be regarded henceforth as phenomenological parameters describing plastic flow of metals. A more extended discussion of this problem is given for example in the work of Hirth [14].

There is however strong evidence that the thermal activation analysis when applied in the proper way, can provide much qualitative information which in turn is very useful in a deeper understanding of the plastic flow of metals and alloys.

Since the plastic deformation of metals is the result of many displacements of many dislocations in the crystal lattice this process is associated with the dynamics of dislocations, i.e. it is time dependent. Under these conditions the plastic deformation rates can be described in terms of a thermally

activated process. Because crystalline materials exhibit a variety of different strain rate and temperature effects there is no simple universally applicable equation to correlate experimentally determined parameters with those which were mentioned above. In addition, many different deformation mechanisms contribute to the net plastic flow at the same time. The most general form of the constitutive relation for the i-th thermally activated dislocation mechanism can be written in the following manner

$$\dot{\gamma}_i = \nu_i(\tau, s_\alpha, T) \exp\left[- \frac{\Delta G_i(\tau^*, s_\alpha, T)}{kT} \right] \qquad (1)$$

where $\nu_i(\tau, s_\alpha, T)$ is called the pre-exponential factor, ΔG_i is the activation free energy, i.e. the net reversible work expended in achieving the activated state of dislocation at constant temperature. The total shear stress and effective shear stress are denoted respectively by τ and τ^*, T is the absolute temperature and k is the Boltzmann constant. Hence, the experimental data show that the thermally activated state can depend not only on the instantaneous values of τ, τ^*, T, $\dot{\gamma}$, but also on the history through which an actual structure of a metal was formed[4]. To account for this effect a number of unspecified structural parameters s has been introduced in equation (1), where $\alpha = 1, \ldots, n$. As will be pointed out later the existence of the structural parameters enable one to introduce a description of structural evolution.

Very frequently eq. (1) is written for the case of instantaneous values

$$\dot{\gamma}_i = \nu_i(\tau, T) \exp\left[- \frac{\Delta G_i(\tau^*, T)}{kT} \right] \qquad (2)$$

and experimental values of the independent variables τ, τ^* and ΔG_i must be obtained from differential tests [15]. To describe strain rate and temperature history effects an evolutionary rate equation must be added to eq. (2) or the

constitutive relation in the form of eq. (1) must be used. For each dislocation mechanism some specific geometric variables are introduced describing structure, for example, density of forest dislocations, geometrics of linear elastic obstacles,[16] etc. A more detailed review of different dislocation mechanisms and geometrics of obstacles involved in each case is given elsewhere [15,17,18,19].

All quantities in equation (1) must be recognized as "averaged" values; this introduces the so called formalism in the approach. However, the number of dislocations or obstacles involved is typically of the order of 10^{10} to 10^{12} cm^{-2}. Hence, a variety of approximations is commonly made in estimating $\dot{\gamma}_i$ for specified thermally activated mechanisms. Usually an element of a dislocation line of length L is assumed on which a net resolved shear stress τ^* is acting; this stress is sometimes called the effective stress. The effective stress τ^*, which assists in successful thermal activation is related to the applied stress τ and athermal stress τ_A through the relation

$$\tau^* = \tau - \tau_A \tag{3}$$

The free energy of activation can be written in a more specific form, see for example [14],

$$\Delta G = \Delta E - T\Delta S + p\Delta V - v^* \tau^* \tag{4}$$

where ΔE is the energy of activation, i.e. energy supplied by the thermal vibration of the lattice, ΔS is the entropy term and p is the hydrostatic component of stress respectively, ΔV is the increment of volume. The activation enthalpy is defined as

$$\Delta H = \Delta E - T\Delta S + p\Delta V \tag{5}$$

Usually the term $p\Delta V$ is neglected, and since the ground state of the activation process can be assumed as zero the deltas can be omitted. Hence

$$H_o = E - TS \tag{6}$$

Introducing eq. (6) into eq. (4) one obtains

$$G = H_o - v^* \tau^* \tag{7}$$

and

$$v^* = - \frac{dG}{d\tau^*} \tag{8}$$

The coefficient v^* has the dimensions of volume and is frequently called the activation volume. The activation volume v^* is a critical parameter in the thermal activation strain rate analysis. This parameter gives the physical dimensions characterizing a thermally activated process, its value shows to what extent the effective stress τ^* helps dislocations surmount a short range barrier.[18] Introducing eq. (7) into eq. (2) and denoting $\nu_i(\tau,T) = \dot{\gamma}_o$ one obtains the activation volume v^* in terms of the instantaneous values of H_o, τ^*, $\dot{\gamma}$ and $\dot{\gamma}_o$

$$v^* = \frac{1}{\tau^*} \left(H_o + kT/\ell n \frac{\dot{\gamma}}{\dot{\gamma}_o}\right) \tag{9}$$

Further consideration will be restricted to the case of the linear elastic obstacle [16]. During successive thermally activated surmounting of the barrier by a dislocation segment L, the effective stress τ^* does work τbLa^*, where La^* is the activation area. Again, the term bLa^* has dimension of volume, and the activation volume in this case will be

$$v^* = bLa^* \tag{10}$$

The pre-exponential factor $\nu_i(\tau, s_\alpha, T)$, sometimes called the frequency factor, is related in most cases to the glide velocity of the mobile dislocation density ρ_m. It can be interpreted as the total area A covered in the average successful thermal fluctuation multiplied by the density of mobile dislocation line segments N. The Schmid factor (orientation factor) is θ and ν denotes

vibrational frequency for an average dislocation line segment. Hence,

$$\nu_i = \theta NAb\nu \quad \text{or} \quad \nu_i = \theta\rho_m b\nu \tag{11}$$

The eq. (11) is analogous to the Orovan's equation [20]

$$\dot{\gamma} = \theta\rho_m b\nu \tag{12}$$

where v is the dislocation velocity.

Under these assumptions the structural parameters s_α in the preexponential factor are θ, N, A and ν. However it is not obvious how these parameters depend upon applied stress τ, temperature T or the history of deformation. The most common assumption is that ν_i is constant during the process of plastic deformation of polycrystalline metals. Further study is needed of this point [21].

For the free energy of activation the structural parameters are as follows: τ^*, τ_A, L and a^* or the activation volume v^*. In the most simplified case, the shear strain rate $\dot{\gamma}$ can be described by Seeger's approximation [22], namely

$$\dot{\gamma} = \theta\rho b\left(\frac{\nu b}{L}\right)L \exp\left[-\frac{H_o - \tau^* bLa^*}{kT}\right] \tag{13}$$

This model approximates conditions that apply when undissociated glide dislocations produce jogs upon intersecting undissociated repulsive forest dislocations assuming the obstacles are arranged in a square array of side L.

It may be once more stressed here that equation (13) seems to be an oversimplification of the real physical picture in which one is specifically concerned with the evolution of the dislocation structure which takes place during plastic straining of a polycrystalline metal. But eq. (13) can be used with success for engineering purposes as an approximate relation between the instantaneous physical parameters. It is interesting to note also that in eq. (2) or (13) the shear strain does not enter explicitly as a physical quantity. From the engineering point of view, it is desirable to know how these physical parameters and

specifically the activation volume v^*, change with strain, and whether they are a unique function of strain; or, in other words, how they depend on the history of deformation. In a previous analysis of this problem for polycrystalline aluminum[4], it was shown that if the model of dislocation intersection which is formulated as eq. (13) is plausible, then L or the density of obstacles is also dependent upon strain rate as well as the history of strain rate $h(\dot{\gamma})$. For this case a general relation may be suggested

$$L = L[\gamma, \dot{\gamma}, (\dot{\gamma})] \tag{16}$$

This relation can be regarded as a general form of an evolutionary equation. The main purpose of this paper is to perform a further analysis of this problem on the basis of new experimental data for polycrystalline aluminum - Fig. 2, and copper - Fig. 3.

3. Analysis of Experimental Data

The analysis of the experimental data is an attempt to provide a basic understanding of the strain rate history effects. The ultimate aim of the analysis is, of course, to identify the dislocation mechanism which is responsible for these effects, however, this is not attempted in the present paper. Unfortunately, at the present time, there is a complete lack of experimental data on strain rate history effects at temperatures which differs from room temperature. In addition, this analysis is limited to the most simple approach to the thermally activated strain rate analysis, in spite of some more refined restrictions discussed in the recent literature[19,21,23,24,25]. Such an approach to the problem may show the main trends which should be followed in the future in a more restrictive manner.

The usual procedure to estimate the strain rate dependence of metals is to measure at constant temperature T the strain rate sensitivity parameter β which is defined as follows

$$\beta = \left(\frac{d\tau}{d\ell n\dot{\gamma}}\right)_T \tag{17}$$

or introducing finite differences in eq. (17) one obtains

$$\beta = \frac{\Delta\tau_s}{\ell n\dot{\gamma}_2/\dot{\gamma}_1} \qquad \text{where } \dot{\gamma}_2 > \dot{\gamma}_1, \quad \Delta\ell n\dot{\gamma} = \ell n\dot{\gamma}_2/\dot{\gamma}_1 \tag{18}$$

The most common practice is to measure β from the constant strain rate tests, however, the proper procedure is to measure β from incremental type tests, especially if it is to have a physical meaning. The value of β is directly related to the activation volume v^*. In order to show this let us differentiate eq. (9).

$$\tau^* dv^* + v^* d\tau^* = kTd\left(\ell n\frac{\dot{\gamma}}{\dot{\gamma}_o}\right) \tag{19}$$

For the case when $\dot{\gamma}_o$ = const., which is a frequent first order assumption, eq. (19) yields

$$v^* = kT\frac{d\ell n\dot{\gamma}}{d\tau^*} - \tau^*\frac{dv^*}{d\tau^*} \tag{20}$$

Using definition (17) the experimental activation volume can be introduced

$$v_e^* = kT\frac{d\ell n\dot{\gamma}}{d\tau^*} \simeq \frac{kT}{\beta}$$

and eq. (20) can be re-written in the following form

$$v^* = v_e^* - \tau^*\frac{dv^*}{d\tau^*} \tag{21}$$

The next common assumption in most of the experimental work is to neglect the second term in eq. (21). But this is unjustified without an analysis of how this term contributes to the total value of the activation volume v^*. To estimate the second term in eq. (21) use will be made of the experimental observation that for different metals (including fcc) having various microstructures, the experimental activation volume v_e^* is proportional to the reciprocal of the

thermally activated component of stress τ^*. In other words a hyperbolic dependence of τ^* on v_e^* is obtained[24], and this relation takes form

$$\tau^* = \frac{w_o}{v_e^*} \tag{22}$$

where $w_o = 3.1 \times 10^{-13}$ ergs[24]. In order to eliminate τ^* in eq. (21), eq. (22) can be differentiated, i.e. $d\tau^* = -\frac{w_o}{v_e^{*2}} dv_e^*$, and $d\tau^*$ substituted into eq. (21), then

$$v^* = v_e^*(1 + \frac{dv^*}{dv_e^*}) \tag{23}$$

This is a differential equation which can be solved and the solution is

$$v^* = v_e^* \ln \frac{v_{oe}^*}{v_e^*} \tag{24}$$

Remembering the definition for v_e^* and β, eq. (24) takes the form

$$v^* = \frac{kT}{\beta} \ln(\beta/\beta_o) \tag{25}$$

or if the strain rate sensitivity is measured at the same increments of strain rates then

$$v^* = \frac{kT}{\beta_s} \ln(\frac{\Delta\tau_s}{\Delta\tau_{so}}) \quad \text{or} \quad \frac{v^*}{v_e^*} = \ln(\frac{\Delta\tau_s}{\Delta\tau_{so}}) \tag{26}$$

where according to Fig. 1 $\beta_s = \frac{\Delta\tau_s}{\Delta \ln \dot{\gamma}}$. Equation (26) can show a range of errors; if the assumption is made that $v^* = v_e^*$, the error will be

$$\chi = \{1 - [\ln(\frac{\Delta\tau_s}{\Delta\tau_{so}})]^{-1}\} \times 100\%$$

Within the region of strains used for aluminum (see Fig. 2) the values of $\frac{\Delta\tau_s}{\Delta\tau_{so}}$ at the lower yield points is about 3.17 which gives $\chi = +13.3\%$, for copper the analogous values are $\frac{\Delta\tau_s}{\Delta\tau_{so}} = 2.190$ (see Fig. 3) and $\chi = -27.5\%$. The numbers confirm to some extent the opinion that the partial differentials can be used to obtain (as a first approach) the activation volume from the incremental tests[15], thus,

$$v^* \simeq v_e^* = kT\left(\frac{\partial \ell n \dot{\gamma}}{\partial \tau}\right)_{\tau^*,T} \tag{27}$$

in this case $dv^*/d\tau^* \simeq 0$ in eq. (20). The activation volume v^* will be regarded henceforth as the experimental activation volume v_e^*.

As is shown schematically in Fig. 1, the experimental results provided by constant strain rate or temperature tests as well as by incremental tests are consistent with this schematic picture for all of fcc polycrystalline metals so far tested. If $\Delta\tau$ denotes the difference at a given value of strain between the two flow stresses obtained at originally constant strain rates $\dot{\gamma}_i$ and $\dot{\gamma}_r$ (or constant temperatures T_i and T_r) then

$$\Delta\tau = \Delta\tau_s + \Delta\tau_h \tag{28}$$

where $\Delta\tau_h$ is the difference in stress at the same level of strain between the incremental stress-strain curve and the curve obtained at the same constant strain rate or temperature. The value of $\Delta\tau_s$ is the elastic response to the increment of strain rate or temperature at a constant structure. For the purpose of further analysis of the experimental data, the following definitions of two activation volumes are introduced, the true activation volume v_s^*

$$v_s^* = kT\left(\frac{\Delta \ell n \dot{\gamma}}{\Delta \tau_s}\right)_{T,\tau^*,\dot{\gamma}_i} \tag{29}$$

and the apparent activation volume v_h^*

$$v_h^* = kT\left(\frac{\Delta \ell n \dot{\gamma}}{\Delta \tau_s + \Delta \tau_h}\right)_{T,\dot{\gamma}_i} \tag{30}$$

Values of the true activation volume v_s^* are obtained from the incremental tests, while values of the apparent activation volume can be obtained from constant strain rate experiments. It is obvious from Fig. 2 and Fig. 3 that v_s^* is always greater than v_h^*. After careful measurements of $\Delta\tau_s$ and $\Delta\tau_h$ at different

initial strains, both activation volumes were obtained, and the results of these measurements are shown for aluminum and copper respectively in Fig. 4 and Fig. 5. In the case of aluminum, values of $\Delta\tau_s$ were obtained by arithematically averaging the upper and lower incremental yield stresses. It may be concluded that for aluminum and copper the values of v_s^* are more than twice as great as the values of v_h^*. This shows again, having in mind the relationship (10), that the true activation area $L_s a^*$ is larger than the apparent activation area $L_h a^*$ deduced from the constant strain rate tests. The activation area undergoes an evolution during a deformation process at a low strain rate; thus, the history of deformation is an important factor in the contribution to the strain rate sensitivity of polycrystalline fcc metals. To illustrate the evolution of the structure, the simplest intersection model will be assumed, i.e. the intersection of two dislocations is completed when $a^* = b$. In this case the activation volume is $v^* = Lb^2$. The density of dislocations is then related to the length of the dislocation segment through the following formula

$$\rho = \frac{1}{L_s^2} \tag{31}$$

Since the apparent activation area $L_h b$ is larger than the true activation area $L_s b$ it means, having in mind how these areas are obtained, that after low strain rate deformation the density of dislocations is lower than after high rate straining to the same level. In other words, the evolution of a structure can be associated with a dislocation annihilation or a dynamic recovery process. In order to perform a qualitative analysis of annihilation the additional relationships will be useful; after differentiation of eq. (31) and $v^* = Lb^2$ one obtains

$$\Delta\rho = -\frac{2\Delta L}{L^3} \tag{32}$$

and

$$\Delta L_s = \frac{\Delta v^*}{b^2}, \quad \text{when} \quad \Delta v^* = v_s^* - v_h^* \tag{33}$$

substituting (31) and (33) into (32) and eliminating L we obtained the following relationship for $\Delta\rho$

$$\Delta\rho = \frac{2b^4}{v_s^{*2}} \Delta v^* \quad \text{or} \quad \Delta\rho = \frac{2b^4}{v_s^{*3}} (v_s^* - v_h^*) \tag{34}$$

and also

$$\Delta\rho = \frac{2b^4}{v_s^{*2}} \left(1 - \frac{v_h^*}{v_s^*}\right)$$

where all the relations hold at constant initial strain γ_i. Here $\Delta\rho$ is understood as the number of dislocations annihilated at a particular value of strain γ_i as compared to two different strain rates $\dot{\gamma}_i$ and $\dot{\gamma}_r$ at which activation volumes v_h^* and v_s^* are experimentally obtained. It is interesting to calculate values of $\Delta\rho$ as a function of initial strain. For this purpose, as a first step, values of $\Delta v^* = v_s^* - v_h^*$, can be obtained on the basis of Fig. 4 and Fig. 5. The results are shown in Fig. 6 and Fig. 7 for aluminum and copper respectively. These results were used to calculate from eq. (34) the number of annihilated dislocations $\Delta\rho$ at different values of γ_i. The results are shown in Fig. 8 and Fig. 9. It appears that at room temperature the number of annihilated dislocations is proportional to the initial strain γ_i which is obtained at constant low strain rate $\dot{\gamma}_i$. This is observed for aluminum as well as for copper. The experimental points imply a linear relationship between $\Delta\rho$ and γ_i and were analyzed using the least squares method. The correlation coefficients appeared to be very close to unity $r^2_{Al} = 0.9970$ and $r^2_{Cu} = 0.9967$; correlation $r^2 = 1$ implies a perfect fit to experimental data. Since the linear relationship

$$\Delta\rho = A + \alpha\gamma_i \tag{35}$$

holds, the coefficient α provides information about the intensity of the annihilation process. These values of α, as indicated in Fig. 8 and Fig. 9 are $\alpha_{Al} = 8.757 \times 10^9$ cm^{-2}; $\alpha_{Cu} = 2.65 \times 10^{10}$ cm^{-2}. If a linear relationship (35) were to hold up to $\gamma_i = 1.0$ (100% shear deformation) then α would indicate the number of dislocations annihilated up to this strain. The constant A will be equal to zero in general, because at $\gamma_i = 0$, the annihilation process starts. This was almost exactly fulfilled in the case of copper for which $A_{Cu} = -0.058 \times 10^9$ cm^{-2}, while for aluminum the value of A_{Al} is relatively greater, $A_{Al} = 0.247 \times 10^9$ cm^{-2}. However, both values of A can be recognized as small see the proportions in Fig. 8 and Fig. 9. It may be also noted that values of α are obtained at constant initial strain rate $\dot{\gamma}_i$, this implies that the annihilation rate is constant as the time of deformation elapses. Then eq. (35) can be re-written in the following form

$$\Delta\rho = A + at \quad \text{where} \quad a = \alpha\dot{\gamma}_i \tag{36}$$

The annihilation rates $a = \frac{d(\Delta\rho)}{dt} = \alpha\dot{\gamma}_i$ are obtained for aluminum and copper when the proper values of $\dot{\gamma}_i$ are introduced into eq. (36). The result is $a_{Al} = 4.378 \times 10^5$ cm^{-2}s^{-1} for $\dot{\gamma}_i = 5 \times 10^{-5}$s^{-1} and $a_{Cu} = 5.47 \times 10^7$ cm^{-2}s^{-1} for $\dot{\gamma}_i = 2.17 \times 10^{-3}$ s^{-1}.

It is of great interest, at the present stage of discussion, to compare the coefficients of annihilation a obtained in this paper with the coefficients of dislocation multiplication M which are usually measured with the aid of an electron microscopy technique. The frequently observed relation for the total density of dislocations is

$$\rho = \rho_o + M_{eff}\gamma, \tag{37}$$

$$\gamma = \text{const.}$$

where M_{eff} is the effective coefficient of dislocation multiplication. Relation (37) also has a strong theoretical background[26]. The effective multiplication coefficient M_{eff} observed in tensile tests for fcc metals at a low nominal strain rate of 10^{-3} s^{-1} is about 10^{11} cm^{-2}. Available measurements[27] on aluminum single crystals and polycrystals indicate that $2M_{eff} = 1 \times 10^{11}$ cm^{-2} (tensile strain ε is substituted in relation (37)). Generally, the figure is higher for polycrystals[26,27]. Here, the effective value of M_{eff} for polycrystalline aluminum is taken[26,27] as $M_{eff} = 4 \times 10^{10}$ cm^{-2}, this value was obtained at the rate of deformation $\dot{\gamma} = 1 \times 10^{-3}$ s^{-1}. Since the annihilation coefficient α was obtained from the incremental and constant strain rate tests performed at two strain rates $\dot{\gamma} = 5 \times 10^{-5}$ s^{-1} and $\dot{\gamma} = 1 \times 10^{-3}$ s^{-1} the effective multiplication coefficient M_{eff} for the strain rate $\dot{\gamma} = 1 \times 10^{3}$ s^{-1} will be

$$(M_{eff})_{dyn.} = (M_{eff})_{stat.} \cdot \alpha \qquad (38)$$

This situation is shown for aluminum in Fig. 10; the initial dislocation density is assumed as $\rho_o = 1 \times 10^{8}$ cm^{-2}. Thus, a consistent picture is found for aluminum. The result is that at the high strain rate of about 10^{3} s^{-1} the effective coefficient of dislocation multiplication is greater than that for low strain rate deformation, the value is

$$\frac{4.87 \times 10^{10}}{4 \times 10^{10}} - 1 = 0.2175.$$

The total density of dislocations is about 22% larger after high strain rate deformation in comparison to a density measured at the same level of strain after low strain rate straining. It can be said also that about 22% of the dislocations are annihilated during deformation at a low strain rate; again, in comparison to a high strain rate deformation. This picture is consistent with

the electron microscopy observations for aluminum[28]. It has been established that the density of dislocations, measured from the misorientation angle between subgrains, is larger after increased strain rates. It has been possible to present the total dislocation density as a function of the strain rate at constant tensile strain $\varepsilon_i = 0.08$ These results, converted into shear strain and shear strain rate, are shown also in Fig. 10. The total densities of dislocations reported in that paper[28] seem to be too low, especially at the low values of strain rate $1.11 \times 10^{-5}\ s^{-1} < \dot{\gamma} < 1.1 \times 10^{-1}\ s^{-1}$, leading to a very low value of the effective coefficient of multiplication M_{eff}. However, the density of dislocations for the strain rate $\dot{\gamma} = 1.1 \times 10^{2}$ agrees quite well to the prediction of Fig. 10. The dislocation density values obtained in the discussed paper[28] were subject to a rather large error, as the authors say, lowering their true value. This error results from imperfection of the subgrain boundary created by the plastic deformation. Moreover, those estimates do not include the dislocations within the subgrains. Although the values of dislocation densities taken from the discussed paper[28] seem to be too low, the general trend is consistent with the present findings for aluminum.

A similar analysis of the experimental data from Fig. 3 for copper can be performed. The first step is to obtain the effective multiplication coefficient M_{eff} for a low strain rate. The experimental data collected for copper[29,30,31], where the total dislocation densities were measured at different values of the tensile strains and at a low strain rate $\sim 10^{-3}\ s^{-1}$ are shown in Fig. 11. The experimental points yield a straight line, i.e. relationship (37) holds. These experimental points[32] were analyzed by the least squares method, the correlation coefficient was $r = 0.9953$, and the values of ρ_o and $2M_{eff}$ are as follows: $\rho_o = 1.505 \times 10^{8}\ cm^{-2}$, $2M_{eff} = 1.846 \times 10^{11}\ cm^{-2}$. For the case of shear deformation this gives the value of $M_{eff} = 9.23 \times 10^{10}\ cm^{-2}$. Having obtained the

effective coefficient of dislocation multiplication for copper H_{eff}, at $\dot{\gamma} \simeq 1 \times 10^{-4}\ s^{-1}$, it is possible to compare its value with the coefficient of annihilation α, and to use eq. (38) to demonstrate their proportions. This is shown in Fig. 12. Again, the result shows that the effective coefficient of dislocation multiplication at the high strain rate $\dot{\gamma} \simeq 3.5 \times 10^{2}\ s^{-1}$ must be greater than that for low strain rate, the value is

$$\frac{11.88 \times 10^{10}}{9.23 \times 10^{10}} - 1 = 0.2871 \quad ,$$

i.e. 29%. The initial dislocation density is assumed to be $\rho_o = 1.5 \times 10^{8}\ cm^{-2}$. Thus, the whole picture for copper is consistent with the results of the analysis for aluminum. Moreover, the values obtained from the present analysis seem to agree with other data obtained with the aid of electron microscopy.

4. An Evolutionary Equation

A question arises as to which is the best way to describe strain rate and temperature history effects in polycrystalline fcc metals. The shape of the incremental stress-strain curves suggests that it is reasonable to assume that during low strain rate deformation at room temperature a dynamic recovery process takes place.[33] In discussing the effect of recovery on mechanical properties and structure, the dislocation processes of particular interest are cross-slip and climb. Both dislocation mechanisms are responsible for creep behavior;[33,34] also the motion of jogged screw dislocation[17] can be included in this category. It may be added that most of the creep mechanisms which can lead to a dynamic recovery process are diffusion controlled.[34, 17] Thus, only cross-slip is thermally activated,[17] but all of them are, of course, rate dependent . It is out of the scope of this paper to review in a detailed manner all possible dislocation mechanisms which could be responsible for dynamic recovery or annihilation of dislocations.

The second possibility which can be offered is the annihilation model based on the concept that under stress mobile dislocations will be immobilized, remobilized and also annihilated. This approach, originally due to Gilman[26] can lead to a proper evolutionary relationship. This point of view can be identified with a proper theory of strain hardening of polycrystalline aggregates.

Because of the nature of strain rate and temperature history effects, both approaches must assume a differential equation as an evolutionary relationship.

Both approaches can be generally represented in terms of effective strain hardening rate.

$$\left(\frac{\partial\tau}{\partial\gamma}\right)_{eff} = \left(\frac{\partial\tau}{\partial\gamma}\right)_{o} + \left(\frac{\partial\tau}{\partial\gamma}\right)_{a} \tag{39}$$

where $\left(\frac{\partial\tau}{\partial\gamma}\right)_{o}$ is the rate of work hardening when no dynamics recovery is occurring, and $\left(\frac{\partial\tau}{\partial\gamma}\right)_{a}$ is the dynamic recovery resulting from dislocation collision and annihilation. If eq. (3) is differentiated with respect to shear strain then one obtains

$$\frac{\partial\tau}{\partial\gamma} = \frac{\partial\tau_A}{\partial\gamma} + \frac{\partial\tau^*}{\partial\gamma} \tag{40}$$

Equation (40) can be split into four terms following eq. (39)

$$\left(\frac{\partial\tau}{\partial\gamma}\right)_{eff} = \left(\frac{\partial\tau_A}{\partial\gamma}\right)_{o} + \left(\frac{\partial\tau_A}{\partial\gamma}\right)_{a} + \left(\frac{\partial\tau^*}{\partial\gamma}\right)_{o} + \left(\frac{\partial\tau^*}{\partial\gamma}\right)_{a} \tag{41}$$

This equation, in a more general form, predicts that the contribution of a dynamic recovery or dislocation annihilation may have two sources, the athermal component of stress τ_A as well as thermally activated component τ^*. The work hardening theories are in favor of $\left(\frac{\partial\tau_A}{\partial\gamma}\right)_{a}$, whereas creep theories suggest that the $\left(\frac{\partial\tau^*}{\partial\gamma}\right)_{a}$ term is dominating. It cannot be excluded that in a certain situation both terms play an important role.

Following Gilman[26], a simple evolutionary equation will be discussed. It is assumed here that dislocations are multiplied with a rate which is proportional to the density of mobile dislocations. Thisis Gilman's original breeding equation, called also the kinetic equation

$$\dot{\rho} = mv\rho_m \tag{42}$$

where ρ is the total dislocation density, m is called the breeding coefficient, and v is the dislocation velocity. In order to include an annihilation process it is necessary to introduce a kinetic equation of annihilation; as a first approach, the rate of annihilation also will be assumed as proportional to the density of mobile dislocations, then

$$\dot{\rho}_a = \frac{v}{\lambda}\rho_m \tag{43}$$

where λ is the average distance traveled before annihilation. The effective rate of dislocation multiplication is

$$\dot{\rho} = \rho_m v(m - \frac{1}{\lambda}) \tag{44}$$

Remembering eq. (12), $\rho_m v$ can be eliminated from eq. (44) and finally the differential equation of structural evolution takes the following form

$$\frac{d\rho}{d\gamma} = \frac{1}{\theta b}(m - \frac{1}{\lambda}) \tag{45}$$

Solution of eq. (45), with the initial condition $\rho = \rho_o$ for $\gamma = 0$, is

$$\rho = \rho_o + \frac{1}{\theta b}(m - \frac{1}{\lambda})\gamma \tag{46}$$

Relationship (45) describes the effective multiplication coefficient M_{eff}. This is analogous to eq. (38) which expresses experimental observations. Thus, it is possible to obtain the average distance before annihilation λ having obtained experimentally values of α,

$$\lambda = \frac{1}{\theta b \alpha} \; ; \; \theta \simeq 1 \tag{47}$$

Since α is not strain dependent, the value of λ is then constant, and for experimental results, see Fig. 8 and Fig. 9, $\lambda_{Al} = 46$ μm; $\lambda_{Cu} = 17$ μm. Having in mind the simplicity of this model, the values given above for λ seem to be reasonable.

To demonstrate some important features of the annihilation process, the second possibility will be discussed, namely the annihilation rate is assumed to be proportional to the total dislocation density

$$\dot{\rho}_a = \eta \rho \tag{48}$$

where η is the coefficient of annihilation. This approach is more plausible for larger strains where the fraction of mobile dislocation is smaller [26]. The effective rate of dislocation accumulation $\dot{\rho}$ is

$$\dot{\rho} = m\frac{\dot{\gamma}}{b} - \eta \rho \tag{49}$$

Again, using eq. (12) one comes to the evolutionary relationship

$$\frac{d\rho}{d\gamma} = \frac{m}{b} - \frac{\eta}{\dot{\gamma}} \rho \tag{50}$$

It is interesting to note that strain rate cannot be eliminated from eq. (50), and must be recognized here as a parameter (not an independent variable). For high strain rates, the second term is perhaps negligible, this term is the dynamic recovery term frequently discussed in literature [35]. The final solution of eq. (50) takes the following form; with the initial condition $\rho = \rho_o$ at $\gamma = 0$

$$\rho = \frac{\dot{\gamma}}{\eta} \left[\frac{m}{b} - \left(\frac{m}{b} - \frac{\eta}{\dot{\gamma}} \rho_o\right) \exp\left(-\frac{\eta}{\dot{\gamma}} \gamma\right)\right] \tag{51}$$

The effective coefficient of dislocation multiplication is

$$\frac{d\rho}{d\gamma} = \left(\frac{m}{b} - \frac{\eta}{\dot{\gamma}} \rho_o\right) \exp\left(-\frac{\eta}{\dot{\gamma}} \gamma\right) \tag{52}$$

This solution has some interesting features; for example

$$\lim_{\dot{\gamma}\to\infty} \left(\frac{d\rho}{d\gamma}\right) = \frac{m}{b} = M_o$$

i.e. at a very high strain rate the recovery term is negligible and the effective breeding coefficient is $M_o = \frac{m}{b}$. For very small plastic strains the following limit holds

$$\lim_{\gamma\to 0} \left(\frac{d\rho}{d\gamma}\right) = \frac{m}{b} - \frac{\eta}{\dot{\gamma}}\rho_o$$

which is analogous to eq. (38). This gives the solution for small strains

$$\rho = \rho_o + \left(\frac{m}{b} - \frac{\eta}{\dot{\gamma}}\rho_o\right)\gamma \qquad (53)$$

or

$$\rho = \frac{m}{b}\gamma - (\eta t - 1)\rho_o \; ; \quad t = \gamma/\dot{\gamma}$$

where t is time of deformation at the strain rate $\dot{\gamma}$. Since the strain rate $\dot{\gamma}$ is assumed to be a parameter, time can enter into eq. (53) explicitly. Solution (51) shows also that the annihilation process is capable of developing an additional rate sensitivity effect. The conclusion is reached that both models discussed so far can, indeed, describe the strain rate history effects.

Another evolutionary equation was recently introduced and discussed in the literature [32] This evolutionary relationship has the following form

$$\frac{d\rho}{d\gamma} = u(\gamma) - A - \Omega\rho \qquad (54)$$

Three main parameters are introduced, i.e. $u(\gamma)$, the coefficient showing the amount of mobile dislocations which are immobilized or annihilated; Ω, the probability for remobilization or annihilation of immobile dislocations; and A, the coefficient of annihilation of mobile dislocations with other mobile dislocations, grain boundaries, etc. This evolutionary relationship does not include a recovery term, since the time factor was eliminated from the basic

assumptions for this model, however, similar treatment as in the first two forms, eqs. (44) and (49) might be used in eq. (54) to include a dynamic recovery.

So far, all discussion of the evolutionary relationship has been limited to the case of a constant temperature. A very basic question arises: how the breeding coefficient m, and more importantly, the annihilation coefficient η or the average path of annihilation λ, are dependent on temperature. It may be exptected that the breeding coefficient should be diminished when temperature rises, and the annihilation coefficient η probably will increase with increasing temperatures. These two opposite trends would intensify the rate history effects (recovery) with increasing temperatures. Since the temperature history effects[1,2] occur, the idea that the thermal vibrations of the lattice take part in the annihilation process cannot be rejected, i.e. the term $(\frac{\partial \tau^*}{\partial \gamma})_a$ is more important in eq. (41).

It will be presently assumed, as it is shown on the basis of the experimental data in Fig. 8 and Fig. 9, that at a constant strain rate and temperature the annihilation rate is constant and equals -a, thus

$$\frac{d\rho_a}{dt} = -a \tag{55}$$

and it is assumed further that this process is thermally activated. The simplest form of temperature dependence will be assumed, namely

$$a = a_o \exp(-\frac{H_a}{kT}) \tag{56}$$

where H_a is an unspecified activation energy for thermally activated annihilation, a_o is the pre-exponentional factor. Introducing eq. (56) into (55) yields the part of the evolutionary relationship

$$\frac{d\rho_a}{dt} = a_o \exp(-\frac{H_a}{kT}) \tag{57}$$

It is understood that the breeding equation (42) holds at the same time; the

subtraction of eq. (42) and (57) gives the evolutionary relationship (58) in the differential form

$$\frac{d\rho}{d\gamma} = \frac{m(T)}{b} - \frac{a_o}{\dot{\gamma}} \exp(-\frac{H_a}{kT}) \tag{58}$$

This equation is very similar to eq. (50), the comparison of both equations gives the result that $\eta(T)\rho \equiv a_o \exp(-\frac{H_a}{kT})$. The evolutionary eq. (58) can be integrated, and solution takes the following form

$$\rho = \rho_o + [\frac{m(T)}{b} - \frac{a_o}{\dot{\gamma}} \exp(-\frac{H_a}{kT})]\gamma \tag{59}$$

Relationship (59) shows a very similar form to solution (50) obtained for the case of small strains. It will be also interesting to demonstrate how the value of $\Delta\rho_a$ which can be measured experimentally is derived from eq. (59). Often experimental results are compared between two or more conditions of deformation, for example, at two different temperatures and at the same strain rate, or, very frequently, vice-versa, as in this paper. Let us call these two states the actual state and the reference state -denoted by star. The difference between densities of dislocation at these two states is

$$\Delta\rho = \rho - \rho^* \tag{60}$$

Thus, from eq. (59) and eq. (60) one obtains

$$\Delta\rho = \frac{\gamma}{b}[m(T) - m(T^*)] - a_o(te^{-\frac{H_a}{kT}} - t^*e^{-\frac{H_a}{kT^*}}) \tag{61}$$

where

$$t = \frac{\gamma}{\dot{\gamma}}; \quad t^* = \frac{\gamma}{\dot{\gamma}^*}; \quad \gamma = \text{const.}; \quad T > T^*; \quad \dot{\gamma} < \dot{\gamma}^*$$

When the parameter $\theta = t \exp(-\frac{H_a}{kT})$ is introduced, and also the following expression is used $\Delta m(T) = m(T) - m(T^*)$; eq. (61) reduces to

$$\Delta\rho = \frac{m(T)}{b}\gamma - a_o(\theta - \theta^*) \tag{62}$$

The parameter θ is frequently used in the creep theories and is called the time modified by temperature.

For the isothermal case, when $T = T^*$ eq. (61) reduces once again to the simplest form, which is the case in the present experiments

$$\Delta\rho = -a\gamma_i\left(\frac{1}{\dot{\gamma}_i} - \frac{1}{\dot{\gamma}_r}\right) \tag{63}$$

To demonstrate strain rate history effects large differences between strain rates must be applied, for the present case between $\dot{\gamma}_i \approx 10^{-4}\ s^{-1}$ and $\dot{\gamma}_r = 7 \times 10^{2}\ s^{-1}$. For such a case, $\frac{1}{\dot{\gamma}_i} \gg \frac{1}{\dot{\gamma}_r}$ and eq. (63) reduces to

$$\Delta\rho = -a\,\frac{\gamma_i}{\dot{\gamma}_i} \quad \text{or} \quad \Delta\rho = -a\gamma_i \tag{64}$$

This is the result from Fig. 8 for aluminum and from Fig. 9 for copper.

5. Discussion and Conclusions

The above considerations show that the evolutionary equation is significant in the description of strain rate and strain rate history effects in fcc polycrystalline metals. It seems also that the contribution of the thermally activated component of stress τ^* to the total strain rate effect of constant strain rates is overestimated in literature. This is caused by the fact that the dislocation annihilation processes were neglected. Having this in mind eq. (3) may be written more precisely, but still in a general form

$$\tau = \tau_A(t,T) + \tau^*(\dot{\gamma},T) \tag{65}$$

To be more precise it will be assumed that the following relation holds everytime[17].

$$\tau_A = \xi G(T)\, b\sqrt{\rho(t,T)} \tag{66}$$

where ξ is a constant factor, $G(T)$ is the temperature dependent shear modulus,

ρ and b have their normal meanings. Inversion of eq. (13) gives

$$\tau = \tau_A + \frac{1}{bL\overset{*}{a}} (H_o + kT\ell n \frac{\dot{\gamma}}{\dot{\gamma}_o}) \tag{67}$$

where $\dot{\gamma}_o$ is the pre-exponential factor. Again, assuming the simplest model of dislocation intersection $\overset{*}{a} = b$, and using eq. (31) together with eq. (66), relationship (67) takes the form

$$\tau = \xi G(T) b \sqrt{\rho(t,T)} \left[1 + \frac{1}{\xi G(T) b^3} (H_o(T) + kT\ell n \frac{\dot{\gamma}}{\dot{\gamma}_o})\right] \tag{68}$$

When one of the evolutionary equations is introduced into eq. (68), say eq. (59), one obtains a complete picture of the strain rate and temperature influences as well as strain rate history and temperature history influences on the flow stress, τ, thus

$$\tau = \xi G(T) b [\rho_o + \frac{m(T)}{b} - a_o t \exp(-\frac{H_a}{kT})]^{1/2} \tag{69}$$

$$\times \left[1 + \frac{1}{\xi G(T) b^3} (H_o(T) + kT\ell n \frac{\dot{\gamma}}{\dot{\gamma}_o})\right]$$

It may be noted that the energy of activation H_o is also temperature dependent through the temperature dependence of the shear modulus $G(T)$[17] .The constitutive relationship (69), even in its simple form, reflects a very complicated nature of the strain hardening of polycrystalline aggregates including strain rate effects. Relations like this may bridge a considerable gap which exists between studies, either experimental or theoretical, of the micro-mechanisms of slow and the formulation of microscopic constitutive relationships. Such an approach is applicable in the solution of many important engineering problems involving rapid straining. However, further experimental work is needed to provide evidence as to which approach to the evolutionary relationship may provide the better description of the real behavior. The incremental experiments of different temperatures are of great importance.

The following conclusions may be derived on the basis of the present work.

i. Strain rate and temperature history effects play a very important role in the plastic behavior of polycrystalline fcc metals.

ii. A dynamic recovery and a dislocation annihilation process are responsible for these effects. The microstructural changes resulting from deformation at different strain rates or temperatures are made evident by a comparison of experimental results which are obtained at constant strain rates or temperatures with those obtained from incremental tests.

iii. A description of strain rate and temperature history effects is possible by a coupling of two relationships. One of these is the relation resulting from the thermally activated process which is currently dominating, while the second is of an evolutionary type. An evolutionary relationship describes the changes in structure during the course of plastic deformation. A few examples of an evolutionary relationship are discussed.

iv. Much experimental work remains to be done to obtain a deeper understanding of the evolutionary processes which occur within the microstructure during plastic deformation of fcc metals at different temperatures and strain rates. The present paper shows that incremental strain rate experiments at different temperatures are of great importance.

Acknowledgement

The results presented in this paper were obtained in the course of research sponsored by the Army Research Office-Durham, under Contract Number DA-ARO-D-31-124-73-G182.

References

1. J. E. Dorn, A. Goldberg and T. E. Tietz, Metals Technology T. P. No. 2445, 1948.

2. W. D. Sylwestrowicz, Trans. ASME, 188 (1958) 617.

3. J. Klepaczko, Arch. Mech. Stosowanej, 19 (1967) 211.

4. J. Klepaczko, J. Mech. Phys. Solids, 16 (1968) 255.

5. S. Joshida and N. Nagata, Trans. JIM, 7 (1966), 273.

6. R. A. Frantz and J. Duffy, J. Appl. Mech. 39 (1972) 939.

7. J. Klepaczko, R. A. Frantz and J. Duffy, Division of Engineering Report, Brown University, 1974 (in preparation).

8. R. A. Frantz and J. Duffy, Division of Engineering Report, Brown University, NSF - GK-26002X/3, 1972.

9. J. Klepaczko, Division of Engineering Report, Brown University, 1974 (in preparation).

10. T. Nicholas, Exp. Mech., 11 (1971) 370.

11. J. D. Campbell and A. R. Dowling, J. Mech. Phys. Solids, 18 (1970) 43.

12. T. Glenn and W. Bradley, Met. Trans., 4 (1973) 2343.

13. J. Duffy, J. D. Campbell and R. H. Hawley, J. Appl. Mech., 38 (1971) 83.

14. J. P. Hirth, Inelastic Behavior of Solids, ed. M. F. Kanineh, et. al., McGraw-Hill, 1970.

15. H. Conrad, J. of Metals, 16 (1964) 582.

16. T. Surek, M. J. Luton and J. J. Jonas, Phil. Mag., 27 (1973) 425.

17. D. Klahn, A. K. Mukkerjee and J. E. Dorn, Proc. Second Int. Conf. on the Strength of Metals and Alloys, Asilomar, California, 1970.

18. J. E. Dorn, Dislocation Dynamics, Ed. A. R. Rosenfield et. al., McGraw-Hill, 1968.

19. A. G. Evans and R. D. Rawlings, Phys. Stat. Sol., 34 (1969) 9.

20. E. Orowan, Proc. Phys. Soc. (London), 52 (1940) 8.

21. T. Surek, M. J. Luton and J. J. Jonas, Phys. Stat. Sol. 57 (1973) 647.

22. A. Seeger, Phil. Mag., 46 (1955) 1194.

23. T. Surek, M. J. Luton and J. J. Jonas, Phil. Mag., 27 (1973) 425.

24. R. W. Armstrong, Indian J. of Scientific and Ind. Res. (in print).

25. P. Rodriguez and P. Dasgupta, Recent Developments in Metallurgical Science and Technology, New Delhi, I. I. M. S., 1972.

26. J. J. Gilman, Micromechanics of Flow of Solids, McGraw-Hill, 1969, p. 189.

27. M. J. Hordon and B. L. Averbach, Acta Met., 9 (1961) 237 and 297.

28. A. Korbel and K. Swiatkowski, Metal Sci. J., 6 (1972) 60.

29. A. R. Bailey, Phil. Mag., 8 (1963) 223.

30. A. R. Bailey (unpublished data), see: J. D. Livingston, Acta Met. 10 (1962) 229.

31. V. Essmann, M. Rapp and M. Wilkens, Acta Met., 16 (1968) 1275.

32. W. Roberts and Y. Bergstrom, Acta Met., 21 (1973) 457.

33. J. J. Jonas, H. J. McQueen and W. A. Wong, Publications of Iron and Steel Institute, No. 108, 1971.

34. A. H. Clauer and B. A. Wilcox, in Mechanical Behavior of Materials at Elevated Temperatures, ed. M. F. Kaninen et. al., McGraw-Hill, 1970.

35. D. J. Lloyd, J. Appl. Phys., 42 (1971), 3910.

Figure Captions

Figure 1 The schematic summary of typical results for fcc metals; a. - increase of strain rate from $\dot{\gamma}_i$ to $\dot{\gamma}_r$ decrease of temperature from T_i to T_r; b. - decrease of strain rate from $\dot{\gamma}_i$ to $\dot{\gamma}_r$ or increase of temperature from T_i to T_r.

Figure 2 Behavior of 1100-0 aluminum under constant low, constant high strain rate, and under-incremental loading in shear[6], strain rate changes from $\dot{\gamma}_i = 5 \times 10^{-5} s^{-1}$ to $\dot{\gamma}_r = 8.5 \times 10^{2} s^{-1}$.

Figure 3 The results of strain rate change for five initial shear strains for copper[9], strain rate changes from $\dot{\gamma}_i = 2.17 \times 10^{-3} s^{-1}$ to $\dot{\gamma}_r \simeq 9 \times 10^{2}\ s^{-1}$.

Figure 4 True and apparent activation volumes for aluminum ; denoted respectively as v_s^* and v_h^*. Data shown as a function of initial shear strain γ_i.

Figure 5 True and apparent activation volumes v_s^* and v_h^* for copper at different initial shear strains γ_i.

Figure 6 Difference in activation volumes $v_s^* - v_h^*$ for aluminum, data obtained from Fig. 4.

Figure 7 Difference in activation volumes $v_s^* - v_h^*$ for copper, data obtained from Fig. 5.

Figure 8 Annihilated amount of dislocations $\Delta\rho$ for aluminum as compared for two rates of deformation $\dot{\gamma}_i = 5 \times 10^{-5}\ s^{-1}$ and $\dot{\gamma}_r \simeq 1 \times 10^{3}\ s^{-1}$ at different shear strains. Solid line obtained by approximation with the aid of the least squares method.

Figure 9 Amount of dislocation annihilation, $\Delta\rho$ for copper, compared for two rates of deformation, $\dot{\gamma}_i = 2.17 \times 10^{-3}\ s^{-1}$ and $\dot{\gamma}_r = 3.5 \times 10^{2}\ s^{-1}$ at different shear strains. Solid line obtained by approximation with the aid of the least squares method.

Figure 10 Total dislocation density as a function of shear strain at different strain rates; solid lines - data from the present paper, •-data obtained from the electron microscopy measurements[28].

Figure 11 Total dislocation densities for copper [29,30,31] as a function of tensile strain ε; data collected by Roberts and Bergström [32]. Solid line is obtained from the analysis by the least squares method.

Figure 12 Total dislocation density for copper as a function of shear strain at two different strain rates, $\dot{\gamma} = 2.11 \times 10^{-3}\ s^{-1}$ and $\dot{\gamma} = 3.58 \times 10^{2}\ s^{-1}$; the initial dislocation density $\rho_o = 1.5 \times 10^{8}\ cm^{-2}$.

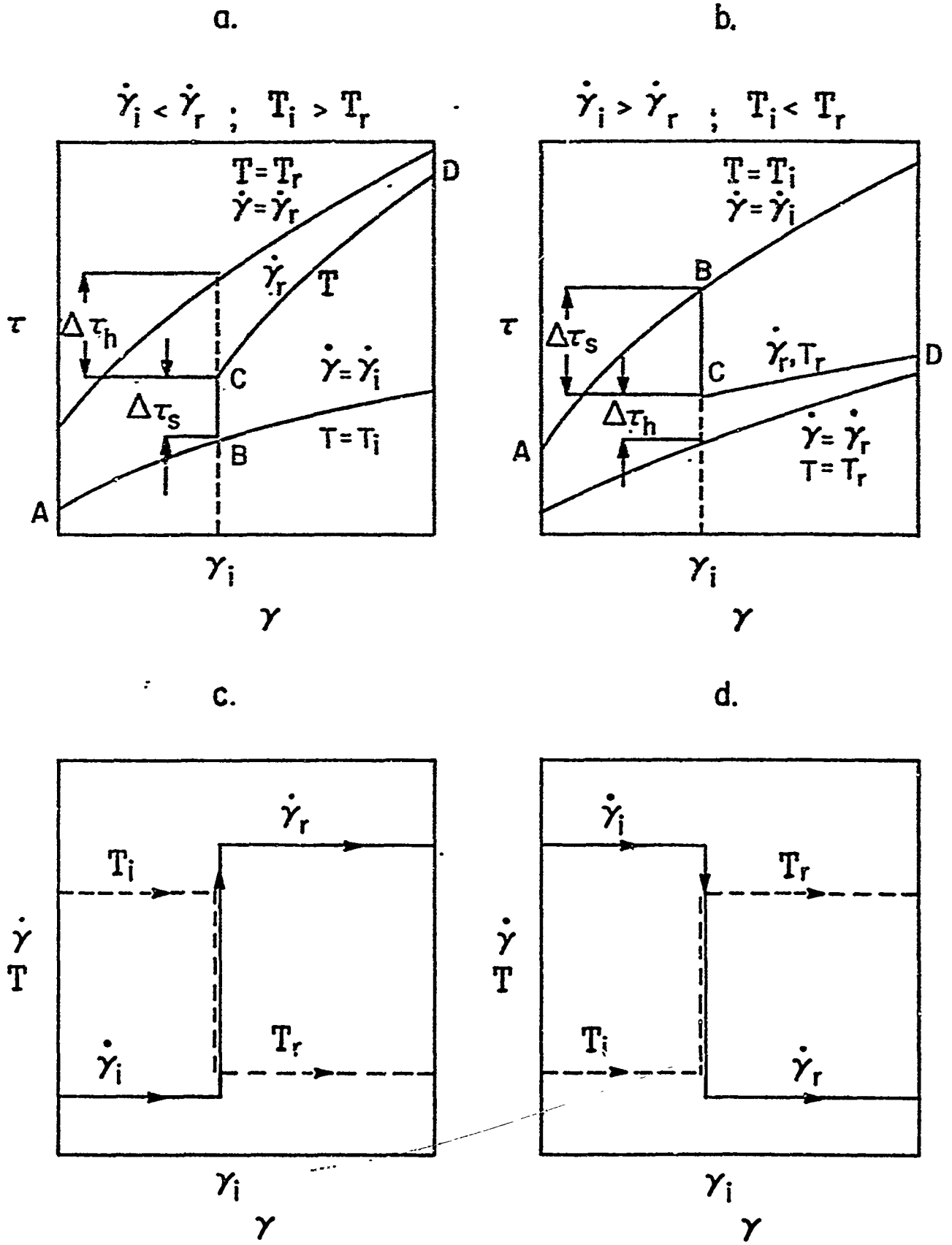
a.
$\dot\gamma_i < \dot\gamma_r$; $T_i > T_r$
$T = T_r$
$\dot\gamma = \dot\gamma_r$
D
$\dot\gamma_r$
T
τ
$\Delta\tau_h$
C
$\dot\gamma = \dot\gamma_i$
$\Delta\tau_s$
$T = T_i$
B
A
γ_i
γ
b.
$\dot\gamma_i > \dot\gamma_r$; $T_i < T_r$
$T = T_i$
$\dot\gamma = \dot\gamma_i$
B
τ
$\Delta\tau_s$
$\dot\gamma_r, T_r$
D
C
$\Delta\tau_h$
A
$\dot\gamma = \dot\gamma_r$
$T = T_r$
γ_i
γ
c.
$\dot\gamma_r$
T_i
$\dot\gamma$
T
$\dot\gamma_i$
T_r
γ_i
γ
d.
$\dot\gamma_i$
T_r
$\dot\gamma$
T
T_i
$\dot\gamma_r$
γ_i
γ

FIG. 1

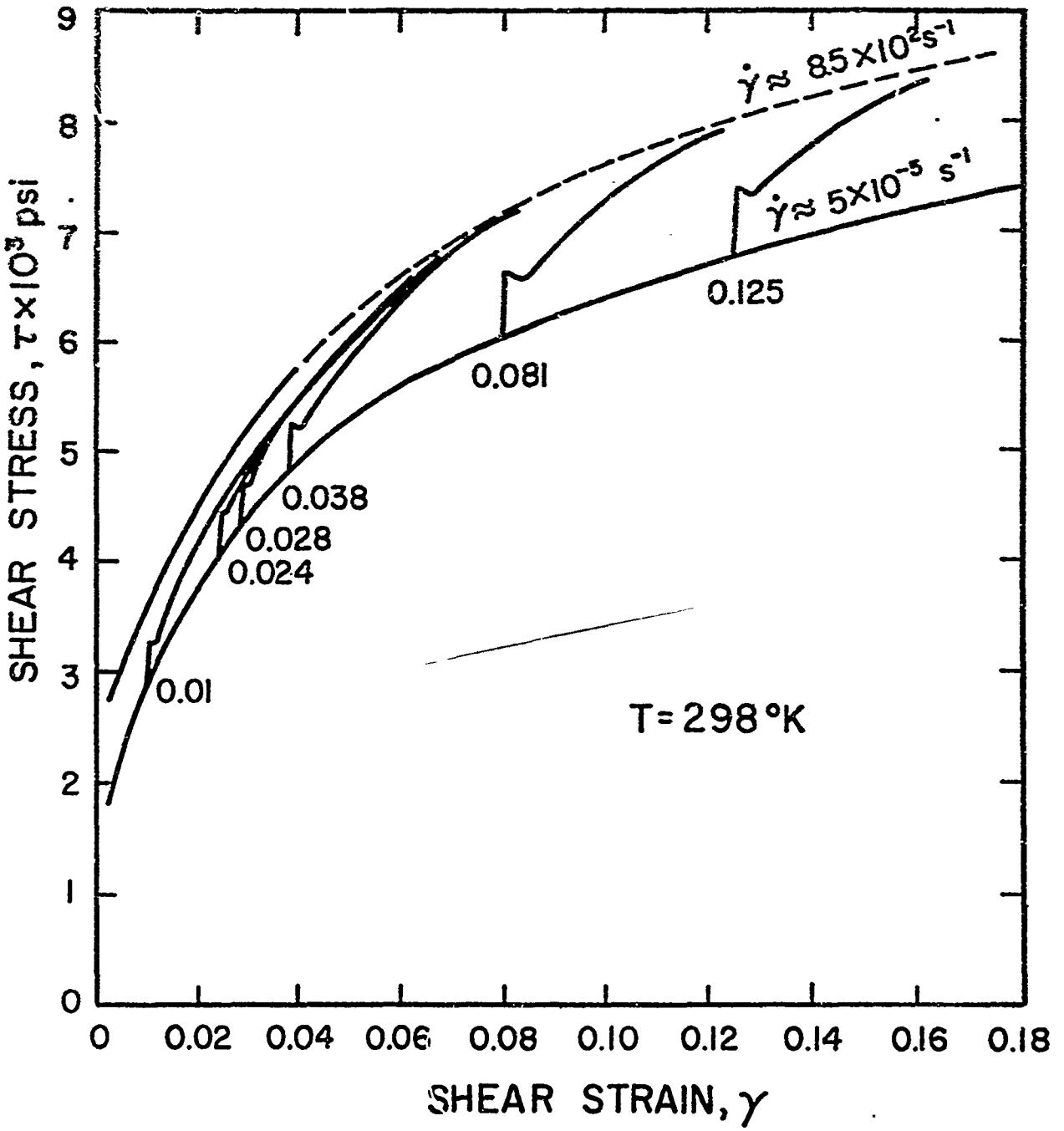
SHEAR STRESS, $\tau \times 10^3$ psi
SHEAR STRAIN, γ
$\dot{\gamma} \approx 85 \times 10^{-2} s^{-1}$
$\dot{\gamma} \approx 5 \times 10^{-5} s^{-1}$
0.01
0.024
0.028
0.038
0.081
0.125
T = 298 °K
0
1
2
3
4
5
6
7
8
9
0
0.02
0.04
0.06
0.08
0.10
0.12
0.14
0.16
0.18

FIG. 2

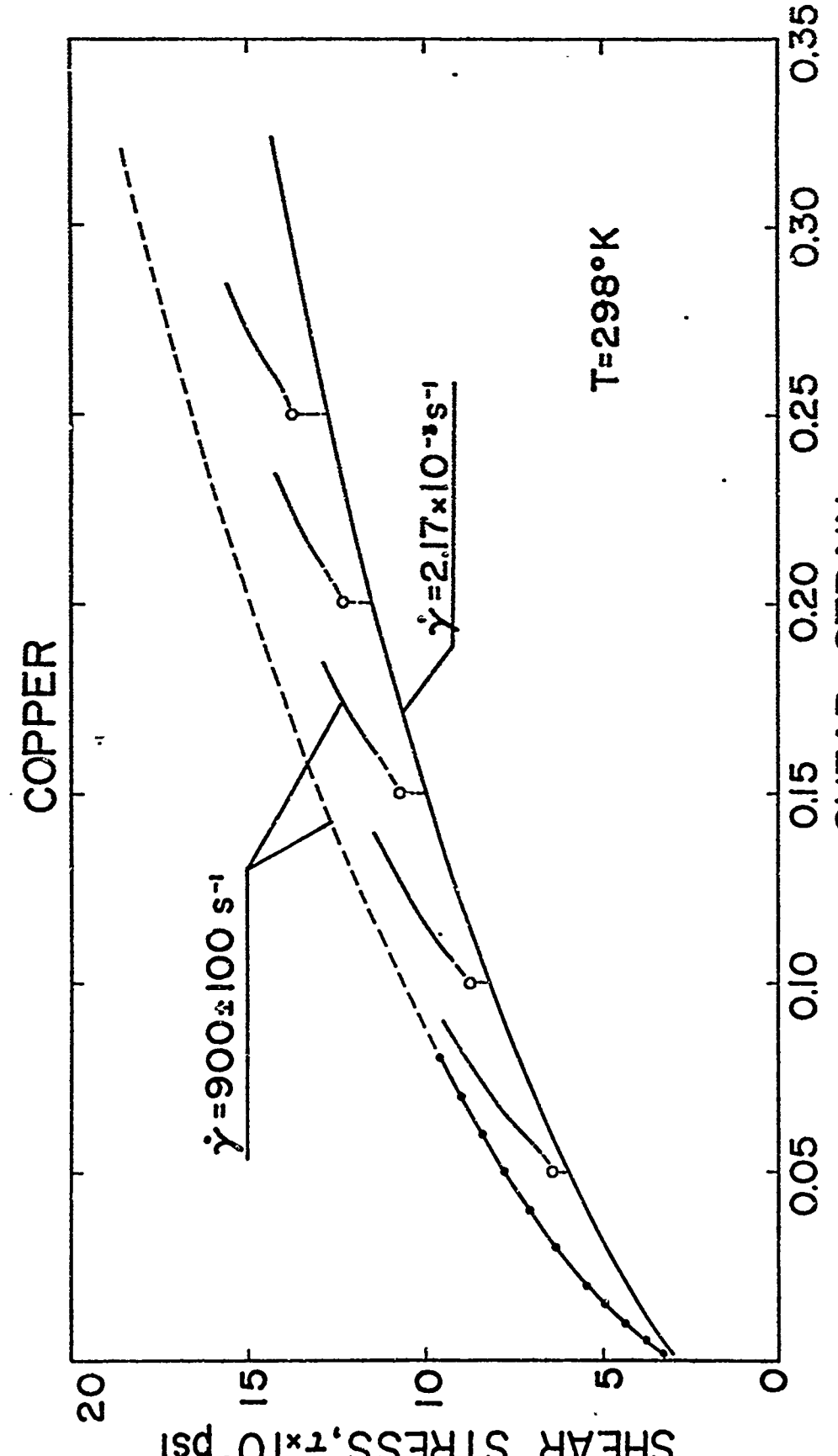
COPPER
T=298°K
$\dot{\gamma}$=900±100 s^{-1}
$\dot{\gamma}$=2.17×10^{-3}s^{-1}
SHEAR STRESS, τ×10^{3} psi
SHEAR STRAIN, γ
0
5
10
15
20
0.05
0.10
0.15
0.20
0.25
0.30
0.35

FIG. 3

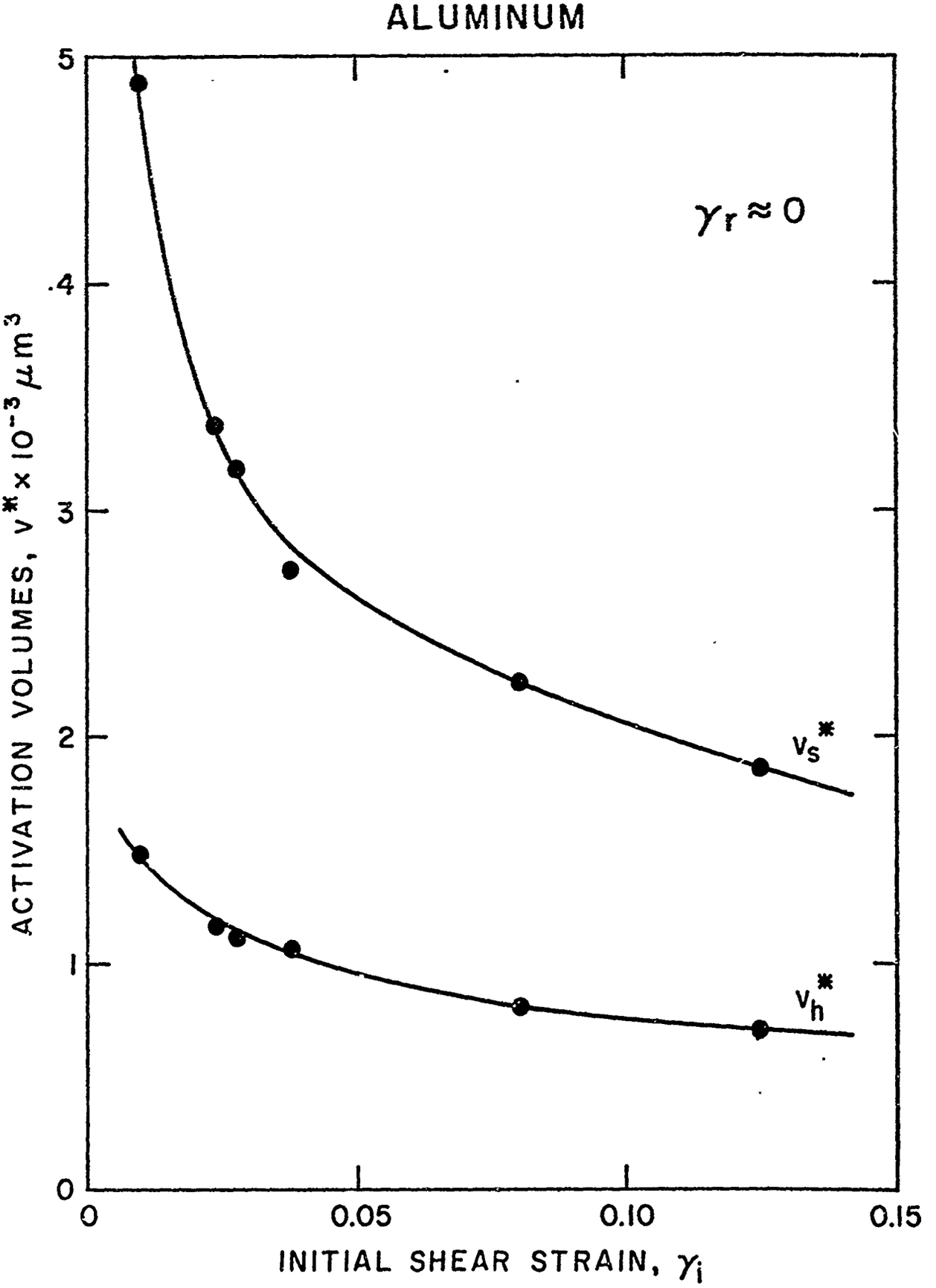
ALUMINUM
$\gamma_r \approx 0$
v_s^*
v_h^*
ACTIVATION VOLUMES, $v^* \times 10^{-3} \mu m^3$
INITIAL SHEAR STRAIN, γ_i
0
1
2
3
.4
5
0
0.05
0.10
0.15

FIG. 4

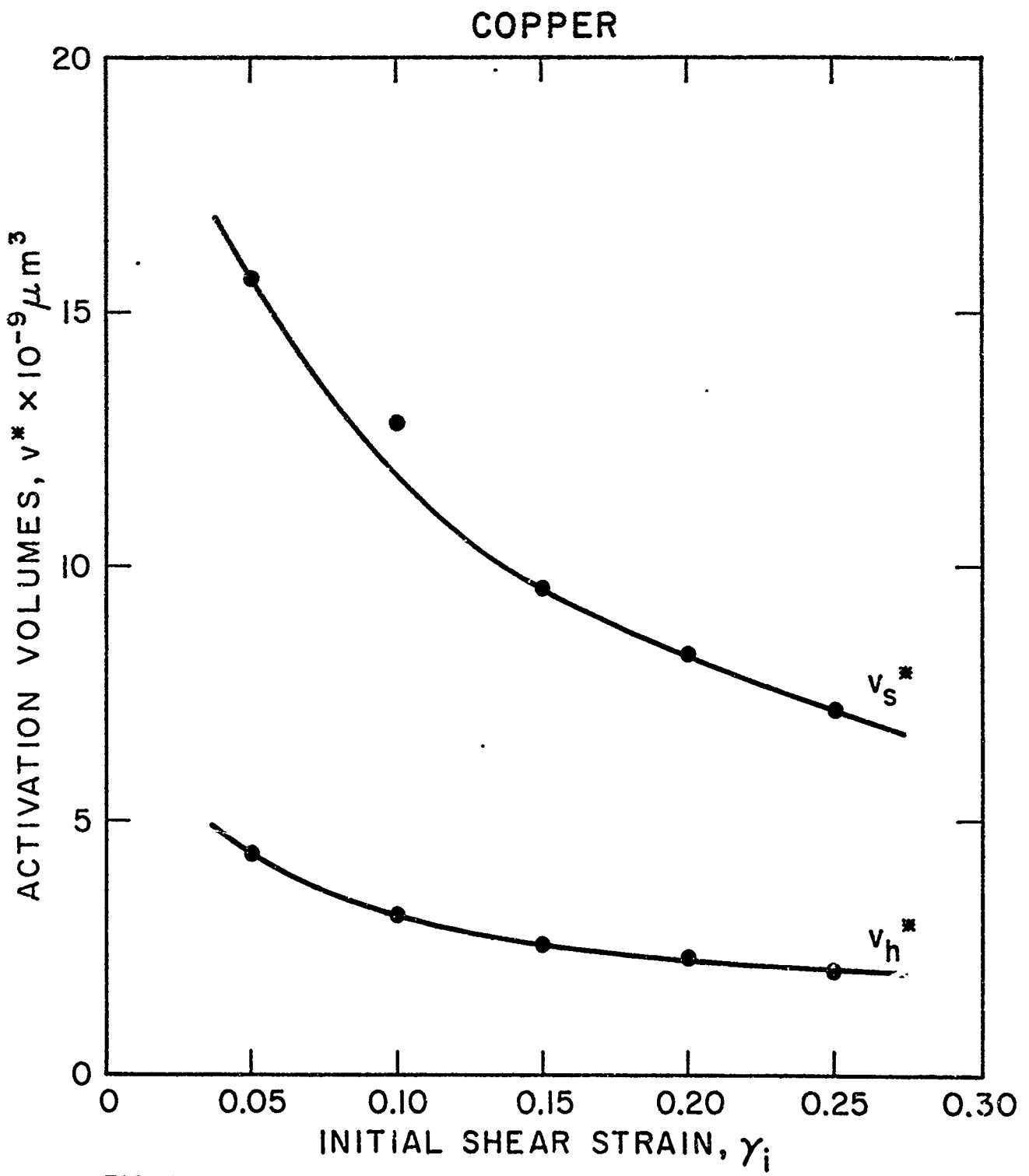
COPPER
20
15
10
5
0
0
0.05
0.10
0.15
0.20
0.25
0.30
ACTIVATION VOLUMES, $v^* \times 10^{-9} \mu m^3$
INITIAL SHEAR STRAIN, γ_i
v_s^*
v_h^*

FIG. 5

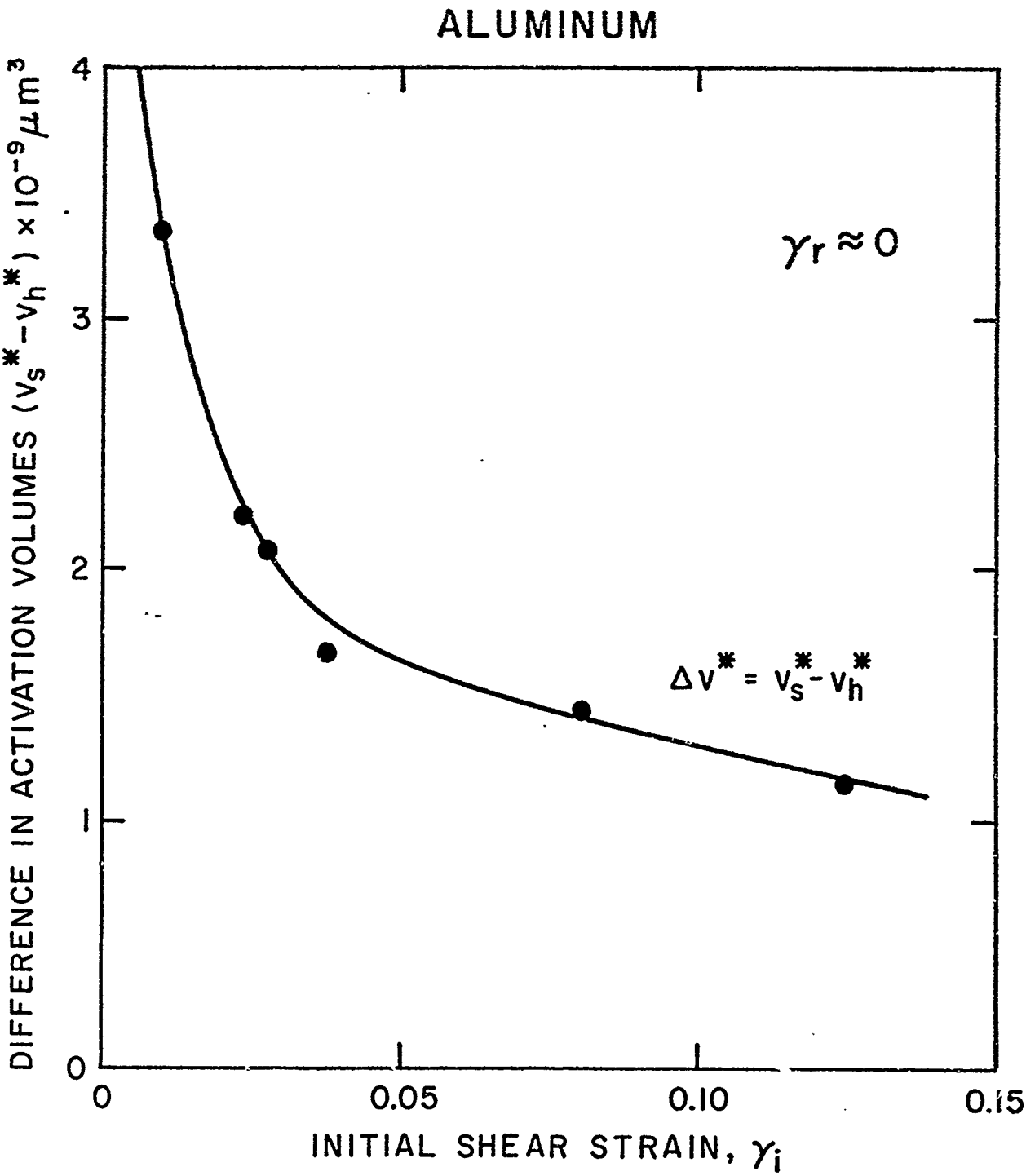
ALUMINUM
DIFFERENCE IN ACTIVATION VOLUMES ($v_s^* - v_h^*$) $\times 10^{-9} \mu m^3$
4
3
2
1
0
0
0.05
0.10
0.15
INITIAL SHEAR STRAIN, γ_i
$\gamma_r \approx 0$
$\Delta v^* = v_s^* - v_h^*$

FIG. 6

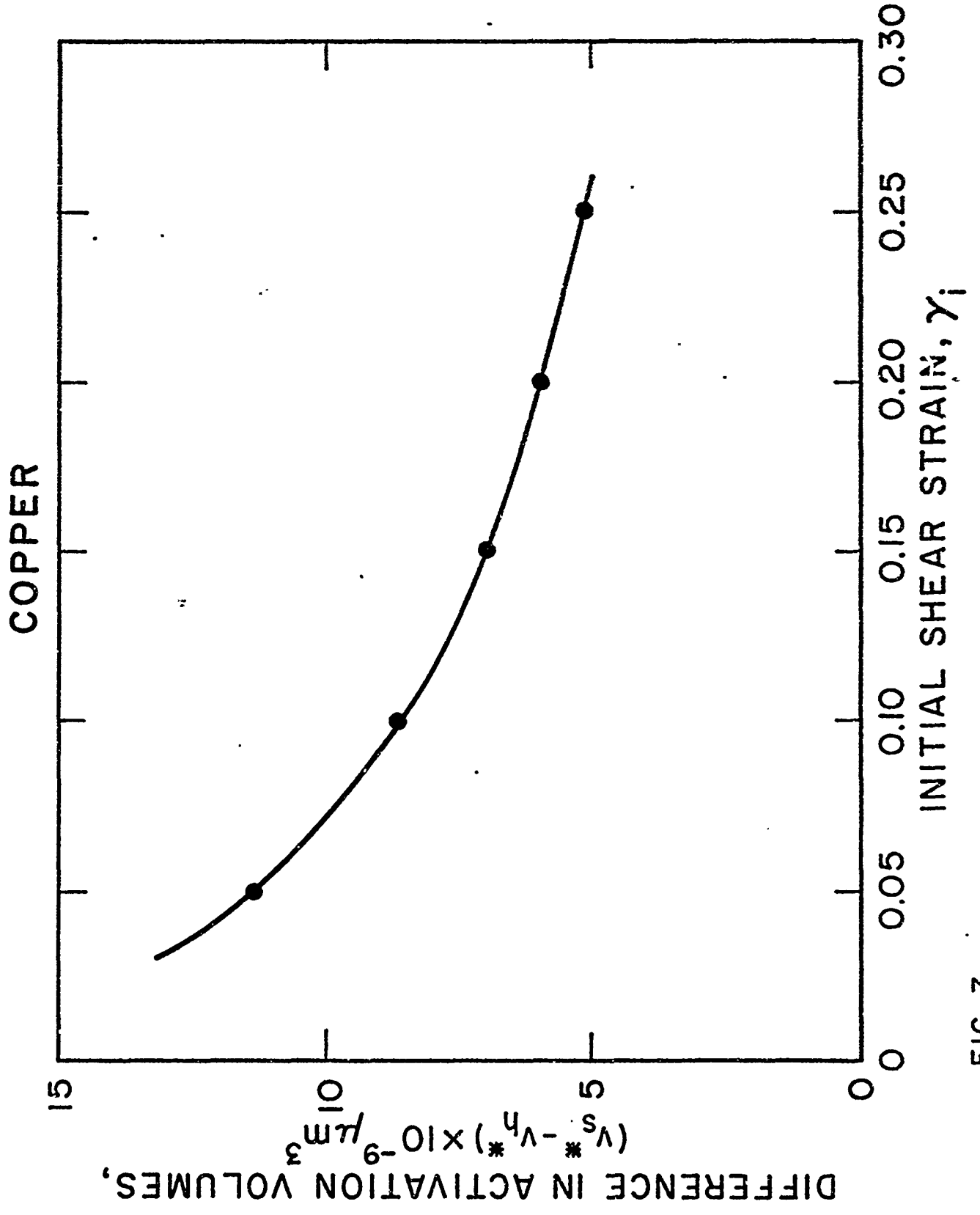
COPPER
INITIAL SHEAR STRAIN, γ_i
0
0.05
0.10
0.15
0.20
0.25
0.30
DIFFERENCE IN ACTIVATION VOLUMES, $(v_s^* - v_h^*) \times 10^{-9} \mu m^3$
15
10
5
0

FIG. 7

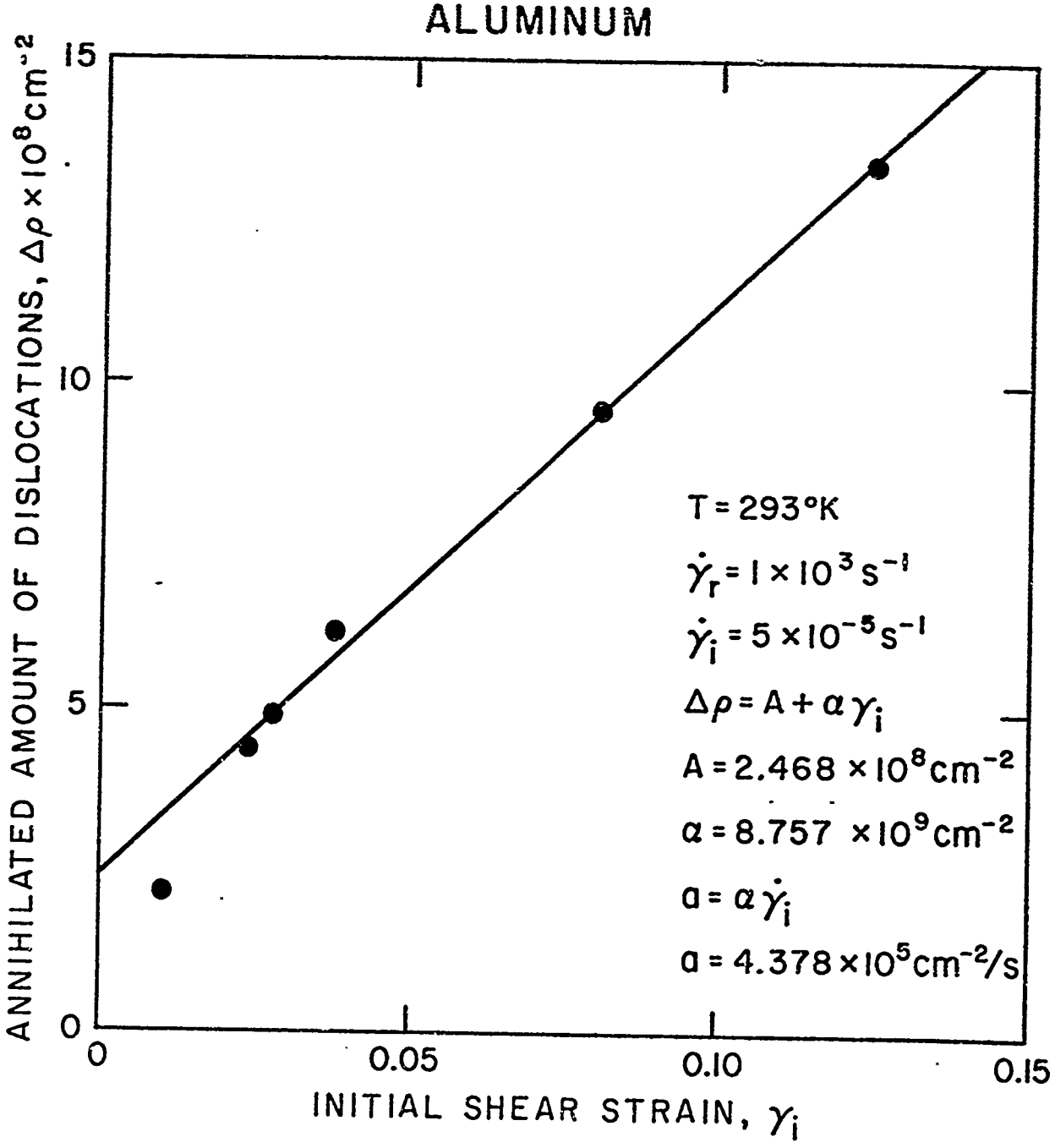
ALUMINUM
ANNIHILATED AMOUNT OF DISLOCATIONS, $\Delta\rho \times 10^8 cm^{-2}$
15
10
5
0
0
0.05
0.10
0.15
INITIAL SHEAR STRAIN, γ_i
T = 293°K
$\dot{\gamma}_r = 1 \times 10^3 s^{-1}$
$\dot{\gamma}_i = 5 \times 10^{-5} s^{-1}$
$\Delta\rho = A + \alpha\gamma_i$
$A = 2.468 \times 10^8 cm^{-2}$
$\alpha = 8.757 \times 10^9 cm^{-2}$
$a = \alpha\dot{\gamma}_i$
$a = 4.378 \times 10^5 cm^{-2}/s$

FIG. 8

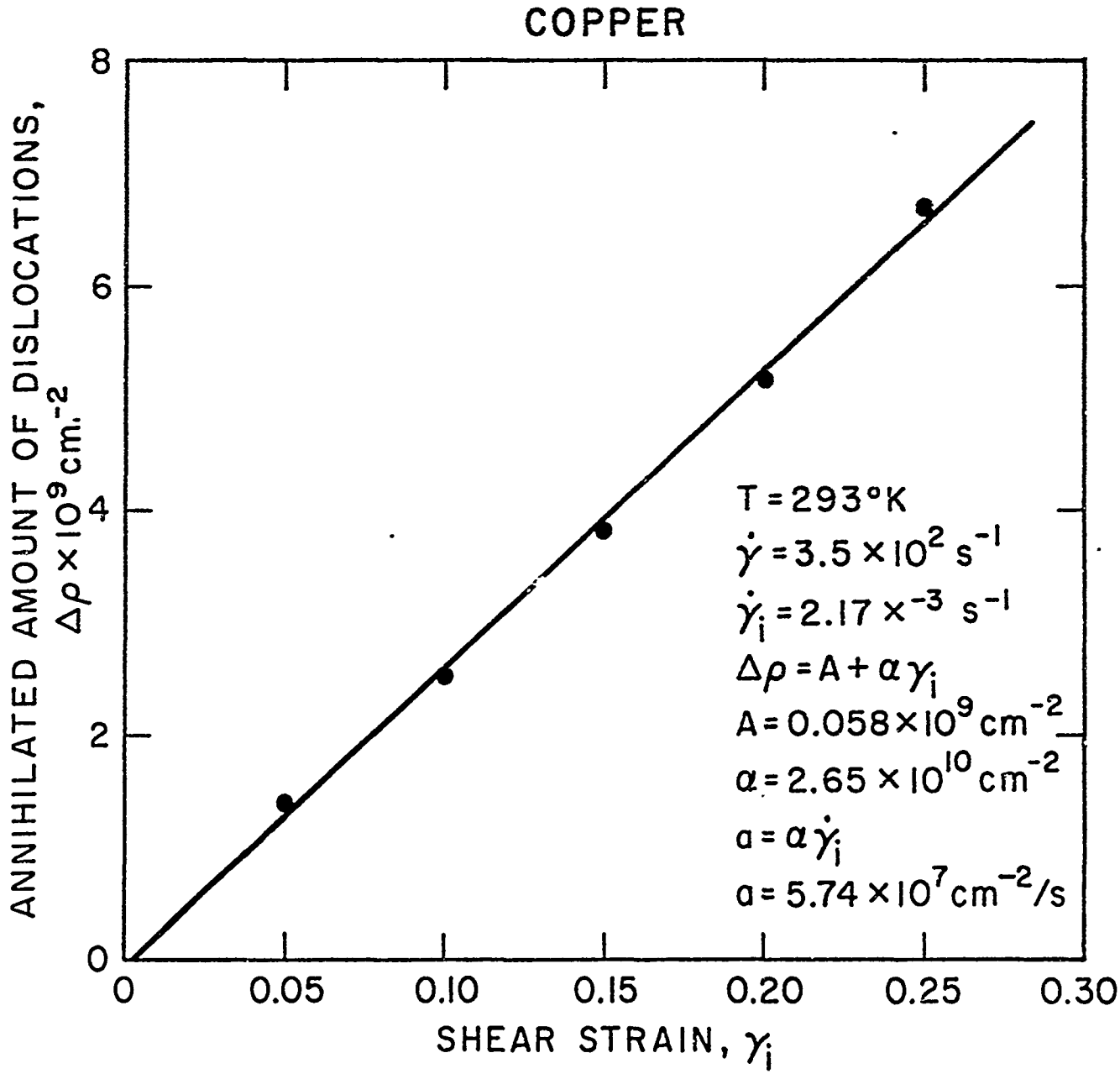
COPPER
ANNIHILATED AMOUNT OF DISLOCATIONS, $\Delta\rho \times 10^9 cm.^{-2}$
8
6
4
2
0
0
0.05
0.10
0.15
0.20
0.25
0.30
SHEAR STRAIN, γ_i
T = 293°K
$\dot{\gamma} = 3.5 \times 10^2 s^{-1}$
$\dot{\gamma}_i = 2.17 \times^{-3} s^{-1}$
$\Delta\rho = A + \alpha\gamma_i$
$A = 0.058 \times 10^9 cm^{-2}$
$\alpha = 2.65 \times 10^{10} cm^{-2}$
$a = \alpha\dot{\gamma}_i$
$a = 5.74 \times 10^7 cm^{-2}/s$

FIG. 9

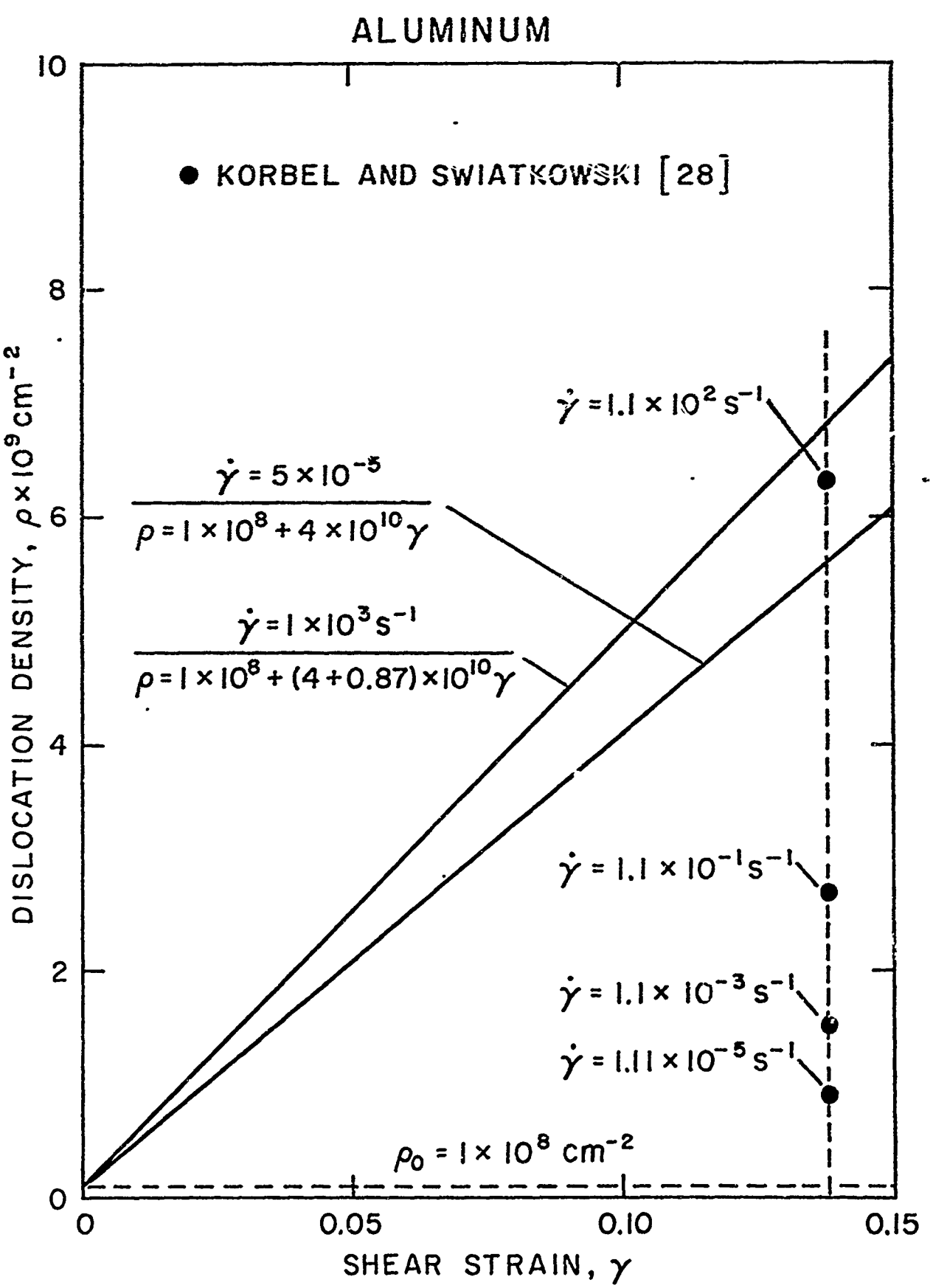
ALUMINUM
KORBEL AND SWIATKOWSKI [28]
$\dot{\gamma} = 1.1 \times 10^{2}\ s^{-1}$
$\dot{\gamma} = 5 \times 10^{-5}$
$\rho = 1 \times 10^{8} + 4 \times 10^{10}\gamma$
$\dot{\gamma} = 1 \times 10^{3} s^{-1}$
$\rho = 1 \times 10^{8} + (4 + 0.87) \times 10^{10}\gamma$
$\dot{\gamma} = 1.1 \times 10^{-1} s^{-1}$
$\dot{\gamma} = 1.1 \times 10^{-3} s^{-1}$
$\dot{\gamma} = 1.11 \times 10^{-5} s^{-1}$
$\rho_0 = 1 \times 10^{8}\ cm^{-2}$
DISLOCATION DENSITY, $\rho \times 10^{9} cm^{-2}$
SHEAR STRAIN, γ
0
2
4
6
8
10
0
0.05
0.10
0.15

FIG. 10

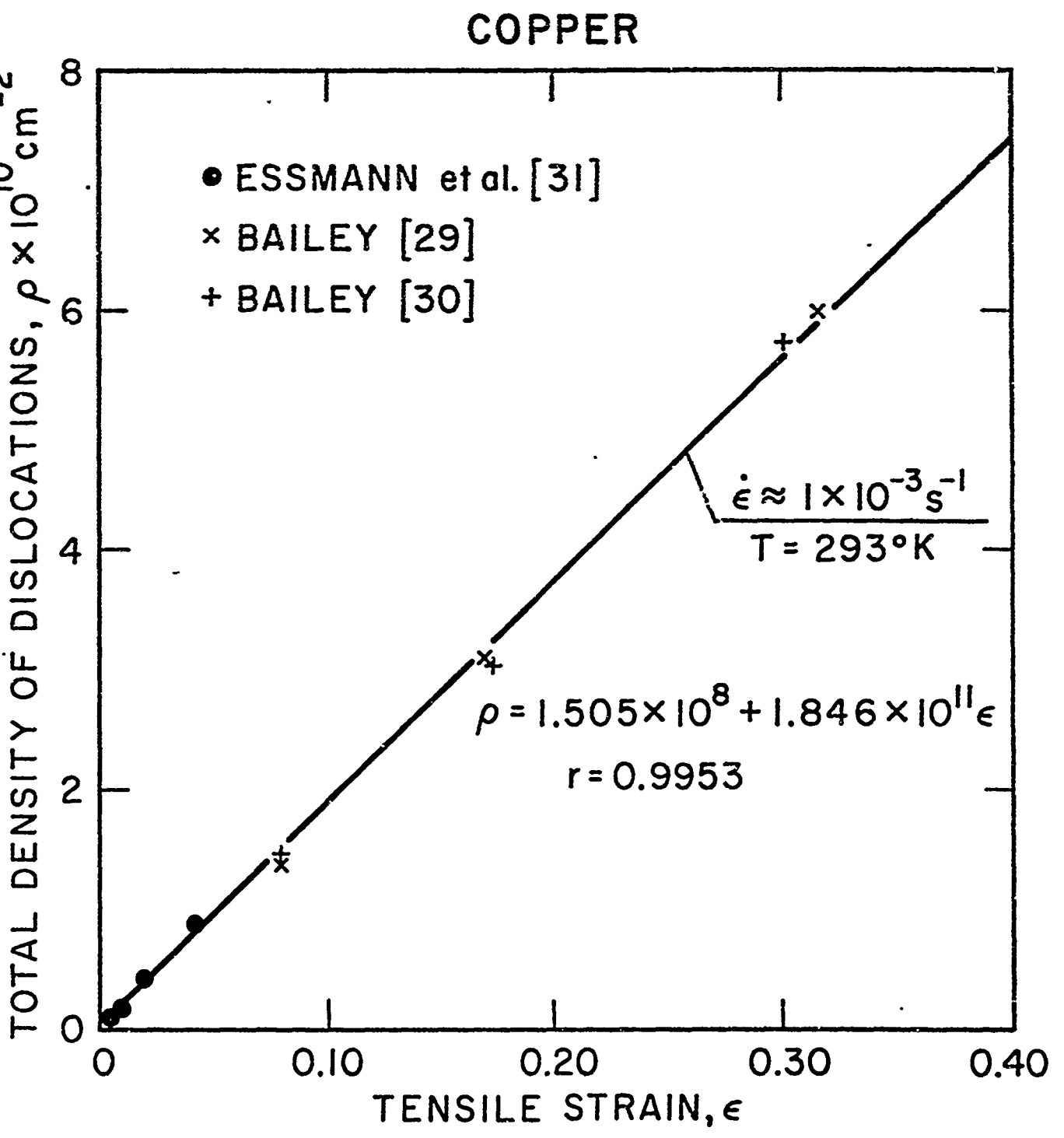
COPPER
TOTAL DENSITY OF DISLOCATIONS, $\rho \times 10^{10}$ cm^{-2}
TENSILE STRAIN, ϵ
0
2
4
6
8
0
0.10
0.20
0.30
0.40
● ESSMANN et al. [31]
× BAILEY [29]
+ BAILEY [30]
$\dot{\epsilon} \approx 1 \times 10^{-3}$ s^{-1}
T = 293°K
$\rho = 1.505 \times 10^{8} + 1.846 \times 10^{11} \epsilon$
r = 0.9953

FIG. 11

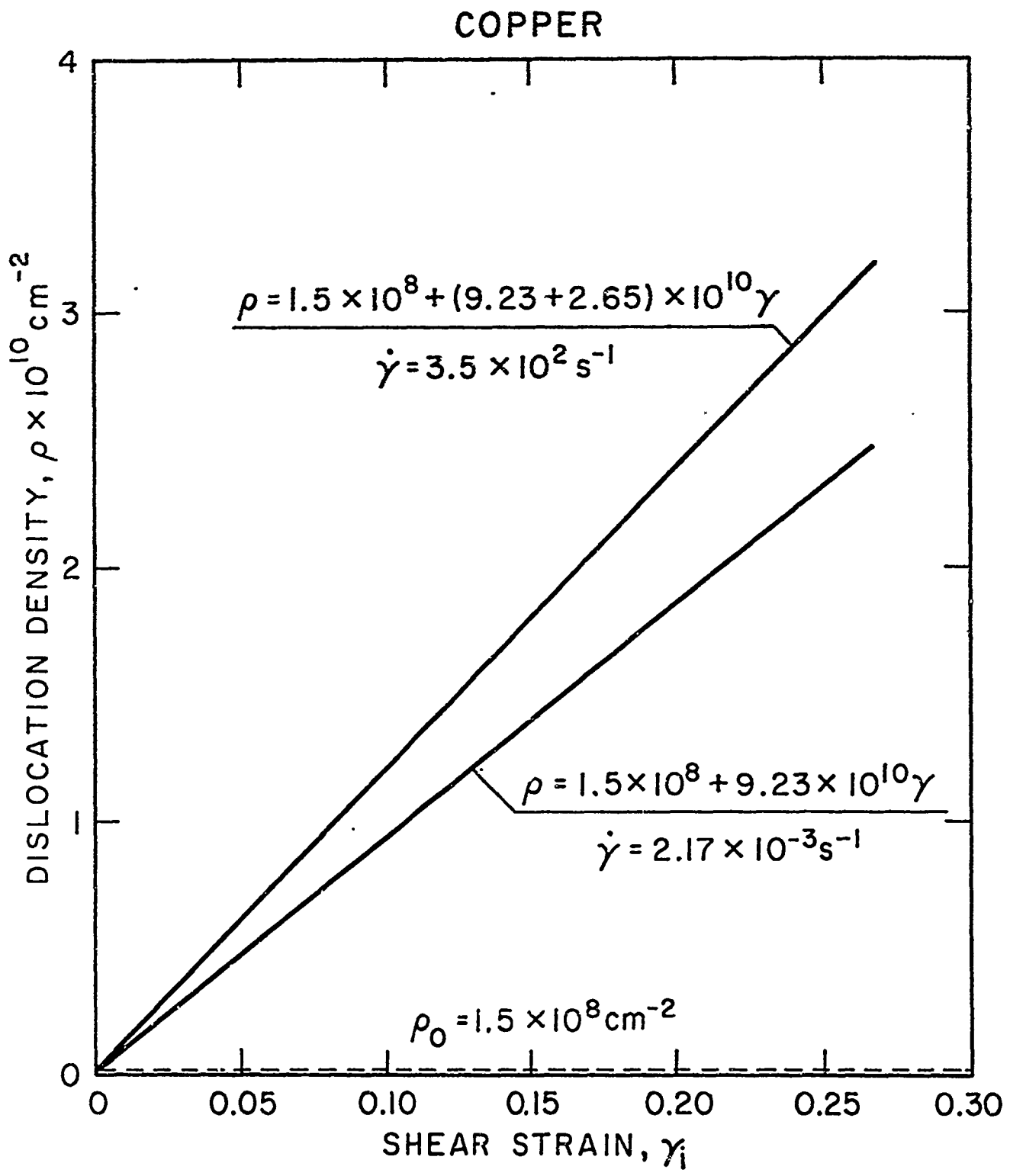
COPPER
DISLOCATION DENSITY, $\rho \times 10^{10}$ cm^{-2}
SHEAR STRAIN, γ_i
$\rho = 1.5 \times 10^8 + (9.23 + 2.65) \times 10^{10} \gamma$
$\dot{\gamma} = 3.5 \times 10^2$ s^{-1}
$\rho = 1.5 \times 10^8 + 9.23 \times 10^{10} \gamma$
$\dot{\gamma} = 2.17 \times 10^{-3}$ s^{-1}
$\rho_0 = 1.5 \times 10^8$ cm^{-2}
0
1
2
3
4
0
0.05
0.10
0.15
0.20
0.25
0.30

FIG. 12